Universidade de Lisboa

Faculdade de Ciências

Departamento de Biologia Vegetal

The role of telomerase on cell proliferation in zebrafish (*Danio rerio*): characterization of a *tert* mutant

Inês Moreira Tenente

Mestrado em Biologia Molecular e Genética

2010

Universidade de Lisboa

Faculdade de Ciências

Departamento de Biologia Vegetal

The role of telomerase on cell proliferation in zebrafish (*Danio rerio*): characterization of a *tert* mutant

Inês Moreira Tenente

Mestrado em Biologia Molecular e Genética

2010

Dissertation advisors:

External advisor: Dr. Miguel Godinho Ferreira, Instituto Gulbenkian de Ciência , Oeiras (in colaboration with Dr. António Jacinto, Instituto de Medicina Molecular – FMUL, Lisboa)

Internal advisor: Prof. Dr. Rui Gomes, FCUL-DBV, Lisboa

Agradecimentos/ Acknowledgements

"São o sonho e o acreditar que fazem o acontecer"

Quero agradecer a todos os que permitiram que atingisse mais esta etapa.

A special thanks to Dr. P. Chapouton, from the German Research Center for Evironmental Health, Germany, for kindly providing the tert^{hu3430} mutant line.

Aos meus orientadores (Dr. Miguel Godinho Ferreira e Dr. António Jacinto), pela confiança que mostraram depositar em mim e nas minhas capacidades. Pela orientação atenta, pelas discussões importantes, pela motivação e entusiasmo. Obrigado por tudo, por me ensinarem a fazer Ciência.

Ao Prof. Rui Gomes, pela sua disponibilidade e orientação. Aos professores e funcionários de Biologia, da Faculdade de Ciências da Universidade de Lisboa, que me acompanharam nestes 5 anos. Guardo boas memórias e ensinamentos. Em especial à Prof. Rita Zilhão, à Prof. Graça Vieira e aos restantes professores da área de Biologia Molecular e Genética e da Biologia de Desenvolvimento, que me apresentaram a um mundo de perguntas fantásticas por responder. Aos restantes professores do meu percurso pré-universitário. À Isabel, à Hélia e a toda a unidade de Biologia Hematopoiética, por ocuparem o vosso tempo comigo no vosso laboratório. Aprendi muito e tenho por vós um grande apreço.

Aos amigos e colegas do IGC, pela ajuda técnica e discussões frutíferas. Em particular, ao pessoal do laboratório de Telómeros e Estabilidade Genómica, por me ensinarem os truques de laboratório e manterem a minha bancada limpa e desocupada! À Maria e à Sofia Azevedo por terem embarcado na aventura deste projecto no início e à Catarina, por acreditar nele, com entusiasmo, na fase final. To everyone at the UMO Unit (IMM), especially to fish people ('little Lara' included) and fish facility technicians. Thanks for all the discussions and for introducing me to this remarkable model. Thanks for all the help during this year. I learned a lot! To everyone at IMM that helped me with technical issues during optimization, thank you!

Aos meus amigos de sempre, Catarina e Carlota, por partilharem comigo este ano tantas experiências e me apoiarem sempre. Ao Jeras, que estando longe continua perto de mim (via Skype). Aos meus colegas de BMG, em especial ao Tiago e à 'pikinina' Ana Luísa, pela amizade em crescimento, apoio, discussões, enfim, tudo! À Guida, Rita, Ana Martins e à Tatiana, por serem assim, amigas, sinceras, e lindas! À Rita, Marco, Aninhas, Sara, Larita e Telmo, pelas aventuras tardias e pela amizade durante este ano. Vai deixar saudade!

À música, que preenche um vazio e de que nunca irei prescindir. Ao Paulo, Vasco e Catherine, por serem culpados de me encher desse bichinho que não desaparece, e pela amizade.

Às pessoas mais importantes, os meus pais e irmãos, e ao Samuel. Por aturarem os meus "stresses", por estarem sempre do meu lado, e por me terem ouvido falar de telómeros, géis e peixes a toda a hora. Ao Samuel um obrigado especial pela ajuda com o MatLab. À minha família e aos que não sendo família é como se fossem. Por me apoiarem sempre. Obrigada!

Resumo

Os telómeros são as extremidades dos cromossomas lineares dos organismos eucarióticos. São regiões de cromatina com propriedades específicas, conferidas pela estrutura do seu ADN e pelas proteínas que a ele estão associadas. Em vertebrados, o ADN telomérico é constituído pela sequência TTAGGG, repetida lado-a-lado um número variável de vezes. Para além de uma região extensa em cadeia dupla, a parte terminal dos telómeros contém uma extremidade projectada a 3', rica em guanosinas, e as proteínas teloméricas estão associadas de forma específica a cada uma destas regiões.

Estas estruturas são essenciais para a manutenção da integridade do genoma, já que conferem protecção face à acção de exonucleases e à acção de enzimas de reparação de danos no ADN. Impedem também a perda de informação genética com a ocorrência da replicação, algo que está relacionado com o 'problema da replicação terminal'. Devido à incapacidade de as polimerases de ADN polimerisarem nucleótidos na ausência de um 'primer', é impossível sintetizar a parte final da cadeia descontínua durante a replicação de moléculas lineares. Isto levaria a que a cadeia de ADN encurtasse, com cada ciclo replicativo, o que conduziria à perda progressiva de informação genética. Os telómeros, sendo estruturas não-génicas, impedem que tal aconteça. Sabe-se que os telómeros encurtam devido não só ao problema da replicação terminal mas também à ressecção adicional, regulada, que dá origem à extremidade 3' projectada. Para que tal não aconteça, as células apresentam mecanismos para alongar os telómeros que podem ser baseados em recombinação entre telómeros (chamados de *Alternative Lengthening Mechanisms* ou *ALT*) ou na acção da telomerase.

A telomerase é constituída por uma componente proteica com actividade de transcritase reversa (Tert) e uma componente de ARN (Terc). Esta nucleoproteína, bastante conservada entre os eucariotas, sintetiza repetições teloméricas a partir do molde que se encontra na componente de ARN, alongando telómeros curtos. A sua produção e actividade são controlados pelas proteínas e demais constituintes dos telómeros e a sua acção depende do estado celular. No Homem, a maioria das células somáticas não a expressa e existe uma correlação entre o tamanho dos telómeros e a idade, sendo os telómeros de pessoas de maior idade mais curtos do que os de pessoas mais jovens. A telomerase é expressa nas células da linha germinal, permitindo a manutenção do comprimento dos telómeros e a transmissão do genoma estável à próxima geração. Esta é também expressa nas células proliferativas de nichos de células estaminais em níveis que não são, porém, suficientes para impedir o encurtamento dos telómeros. As células somáticas não podem ser propagadas em cultura indefinidamente. Sabe-se que em cultura dividem um limitado número de vezes após o qual entram num estado de senescência. Este 'limite de Hayflick'

está relacionado com o facto de os telómeros encurtarem com cada divisão celular. Os telómeros criticamente curtos conduzem à activação de 'checkpoints' dependentes de P53 e outros supressores de tumores, de modo a impedir a progressão do ciclo celular. Deste modo, as células sofrem uma série de alterações que caracterizam a senescência celular ou entram num processo apoptótico. Se tal não acontece, desencadeia-se uma resposta de reparação de danos no ADN, o que leva a instabilidade cromossómica, com a ocorrência de ciclos de fusões entre cromossomas e quebras no ADN e, em último caso, contribui para o surgimento de tumores.

É possível encontrar células senescentes em tecidos. Dado que a maioria das células somáticas não expressa telomerase é possível que o declínio na manutenção do funcionamento dos órgãos e funções biológicas, característico do processo do envelhecimento, esteja relacionado com a incapacidade de proliferação causada pelo encurtamento dos telómeros. Existem algumas doenças humanas que se manifestam em problemas na manutenção dos tecidos, envelhecimento precoce e tempo de vida diminuído. Uma destas doenças, a Disqueratose Congénita, é causada por mutações em componentes da telomerase, o que apoia o papel do encurtamento dos telómeros no processo do envelhecimento, juntamente com o facto de algumas variantes da proteína Tert estarem relacionadas com maior longevidade. Longevidade é o tempo em que é possível a um organismo manter as funções celulares, prevenindo alterações associadas com o envelhecimento. Apesar de o papel dos telómeros na senescência celular ser já reconhecido como importante, o seu papel no envelhecimento e longevidade permanece em investigação.

Estudos em ratinho, com vista a compreender o papel dos telómeros nestes processos, mostraram que a ausência da telomerase causa fenótipos de envelhecimento, como a degeneração de tecidos proliferativos, infertilidade e incapacidade de cicatrização de feridas, acompanhados de alterações citogenéticas de fusões e aneuploidias. No entanto, o ratinho apresenta várias características específicas que o afastam da realidade no Homem. São precisas gerações de cruzamentos entre ratinhos *knock out*, em que os seus telómeros são artificialmente encurtados a um ponto crítico, para que surjam fenótipos. Assim, o eixo telómeros/telomerase não parece ser fundamental para o controlo da proliferação celular e manutenção dos tecidos, ao contrário do que parece acontecer em humanos.

O peixe-zebra (*Danio rerio*) tem sido apresentado como um novo modelo de envelhecimento, e neste âmbito, poderá ser um bom modelo vertebrado alternativo para estudar o papel dos telómeros e da telomerase na proliferação celular e homeostasia de tecidos com o envelhecimento. Este modelo possui várias vantagens específicas: é fácil e barato de manter, o que permite seguir muitos indivíduos; envelhece gradualmente e manifesta características semelhantes às dos humanos; expressa vários marcadores

celulares de senescência que permitem a procura de genes relacionados com o envelhecimento em larga escala; e é um modelo de excelência para manipulação genética e criação de transgénicos para microscopia em tempo real. O peixe tem a capacidade de regenerar quase todos os seus órgãos, ao contrário dos humanos, num processo que depende altamente de proliferação celular, e a expressão da telomerase tem sido apontada como uma das características necessárias para que tal aconteça. Tem também telómeros mais curtos que o ratinho, menor actividade da telomerase e várias observações apontam para um papel da manutenção dos telómeros na proliferação celular e sua implicação no processo de envelhecimento do peixe-zebra.

Neste contexto, pretendeu-se caracterizar um mutante em peixe-zebra, em que a actividade da telomerase foi abolida (*tert*^{hu3430}).

Determinou-se o tamanho médio dos telómeros de mutantes, em comparação com indivíduos selvagens, através da técnica de restrição dos fragmentos terminais seguida de hibridação Southern. O peixe-zebra parece ter, de facto, telómeros curtos, de cerca de 7 Kb, e o mutante apresenta logo aos 6 meses de idade uma diminuição significativa do tamanho dos telómeros no tecido da barbatana caudal, que não é especialmente proliferativo. Isto indica que a telomerase pode ser um mecanismo fundamental para a manutenção dos telómeros neste organismo. Os fenótipos apresentados são consistentes com um papel da telomerase e dos telómeros na proliferação celular e manutenção dos tecidos proliferativos do adulto (intestino, retina, músculo esquelético, brânquias, intestino e gónadas) com o tempo. Uma das primeiras consequências, associada à degeneração das gónadas, é a infertilidade dos machos e, mais tarde, das fêmeas. Embriões homozigóticos mutantes sem contribuição maternal são inviáveis, e apresentam fenótipos variados consistentes com problemas na proliferação celular e/ou apoptose. Assim, a telomerase parece ser fundamental em vários fenómenos que dependem da proliferação celular, em peixe-zebra.

Estes resultados aproximam-se da realidade em humanos, e apoiam a utilização do peixe-zebra como modelo vertebrado alternativo para compreender qual o papel dos telómeros no processo de envelhecimento, determinação de longevidade, e também para modelação do papel dos telómeros e da telomerase no cancro e no processo regenerativo.

Palavras-chave: telómero, telomerase, peixe-zebra, *Danio rerio*, senescência, envelhecimento, proliferação celular, células estaminais; células estaminais do adulto.

Abstract

Telomeres, the tips of linear eukaryotic chromosomes, are responsible for protecting chromosome ends from exonucleases and DNA repair events. Together with the enzyme telomerase, they provide a way to elongate telomeres, preventing loss of genetic information with replication due to the end-replication problem and to additional resection of the 5' end. The progressive shortening of telomeres in the absence of telomerase, or other recombination-based mechanisms, leads to cellular senescence and it is hypothesized that this could be responsible for organismal ageing.

Zebrafish has been proposed as a promising vertebrate ageing model. It ages gradually and display many cellular features common to human senescence. It is currently used for the study of age-dependent changes in various organs, such as the muscle, skeleton and the eye. In contrast to inbred mice, they possess shorter telomeres of the same length of humans (5-10kb), which suggests similar mechanisms in the regulation of cell proliferation by telomeres.

An early nonsense mutation in telomerase component gene *tert* ($tert^{hu3430}$) results in fish that exhibit shorter telomeres observable by 6 months of age. This points telomerase as a fundamental mechanism for telomere maintenance in this organism, in contrast to inbred mice models. The phenotypes are consistent with a role of telomerase in cell proliferation and tissue maintenance in the adult, with impaired organ renewal and function leading to infertility and a decline in health status and precocious death by 1 year of age. A role for telomerase on cell proliferation is also evident on the developmental defects of maternal zygotic mutant embryos that make them unviable.

These results support the use of zebrafish as an alternative animal model for the role of telomeres and telomerase on cell proliferation events like development and regeneration, and tissue turn-over degeneration, which occurs during the ageing process.

Keywords: telomere, telomerase, zebrafish, *Danio rerio*, senescence, ageing, cellular proliferation, stem cells, adult stem cells.

Index

Introduction

1. Telomere structure and function

Telomeres (*Gr. telos* (end); *meros* (part)) are the chromosome components that stabilize its ends. Located at the tips of chromosomes, their importance was left unaddressed until Muller and McClintock[1,2] independently concluded that these terminal structures have unique properties that protect chromosomes from rearrangements and deleterious fusion events. Telomeric DNA is constituted by tandem arrays of G-rich motifs ($(TTAGGG)_n$ in vertebrates) with a 3' overhang at the end. This structure is accompanied by a number of telomere-associated proteins (Figure 1) that bind either to specific sequences within double-stranded or single-stranded regions or to other telomeric proteins. These are responsible for telomere-specific properties and functions. Besides conferring protection, telomeres are essential for controlling terminal replication of linear chromosomes[3,4,5,6].

In mammals, this nucleoprotein complex on telomeres is called *shelterin*, with TRF1 and TRF2/RAP1 proteins lying on the double strand region, POT1/TPP1 on the single-stranded G-rich DNA and TIN2 bridging these two components (Figure 1)[7,8,9]. So far, most eukaryotes present an evident structural and functional conservation of telomere components[10]. Although telomere length varies widely both between and within species[10], this conservation supports the importance of telomeres and of the mechanisms responsible for maintaining their function on cellular and organism viability.

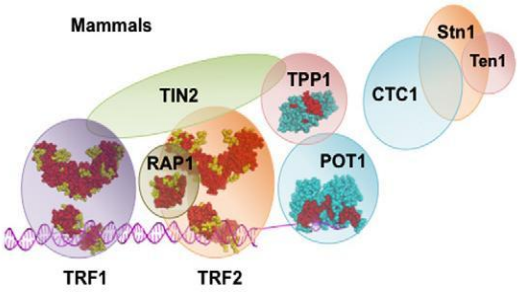

Figure 1: The mammalian *shelterin* complex at telomeres[7].

It has recently become apparent that the chromatin at telomeres has also specific features that play an important role in telomere function. Non-coding RNAs transcribed from telomeres were also recently identified to play a role in telomere maintenance and regulation[11,12,13,14]. The discovery of this Telomere Repeat Associated Transcription (TERRA) changed the view of telomeres as transcriptionally silent, inert regions and, together with new insights on telomeric chromatin regulation and DNA methylation patterns, reinforced the view of telomeres as highly dynamic entities[9,15].

2. The end-replication problem and telomere elongation mechanisms

The end-replication problem was shown by Olovnikov[16] and Watson[17] in the 1970s, at the time of the discovery of the mechanism of DNA replication. In the assumed replication model, DNA polymerases require a 3'OH primer to start incorporating nucleotides, usually provided by primases. In the case of linear DNA replication[17], this would mean that the very end of DNA molecules could never be replicated, therefore leading to an erosion of chromosomes with ultimate loss of genetic information in dividing cells (Figure 2). Without an elongating mechanism, mammalian telomeres shorten at a rate of 50–200 bp/ per population doubling (PD)[18] and not at 3 bp/PD as predicted by the end-replication problem[19]. This higher rate of telomere attrition comes from additional resection mechanisms (Figure 2) that involve enzymes from double strand break repair pathways and is regulated by telomeric proteins like POT1[20,21].

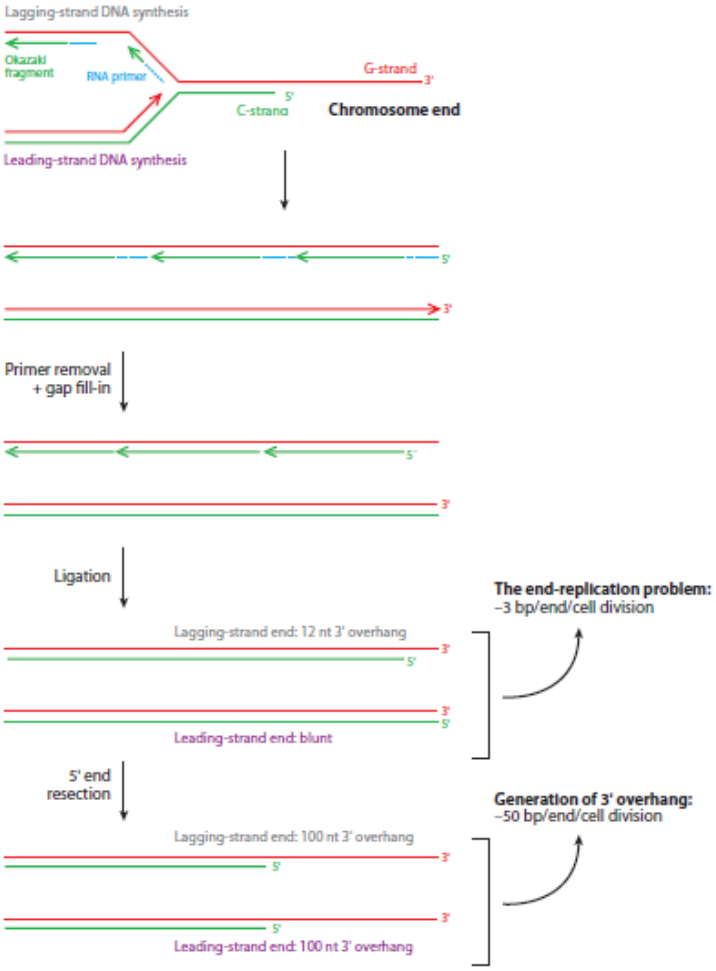

Organisms display various strategies of dealing with this problem. However, in most eukaryotes. telomeres and its associated mechanisms evolved to keep chromosome ends and avoid loss of genetic information[22].

Figure 2: Telomeres shorten with replication in the absence of telomere-elongating mechanisms (adapt.[23]).

- **Telomerase: a solution to the problem**

Blackburn started an important row of experiments that conduced to the discovery of telomerase[24]. Her group cloned *Tetrahymena* telomeres onto a linear plasmid construct from yeast provided by Szostak[25] and sequenced them after some culture time. For their surprise, they found that yeast-specific sequences were being added to the terminus of the initial telomeric sequences from *Tetrahymena*[26]. At the time some theoretical models for elongation of telomeres, which were based on recombination events, were already proposed.

These mechanisms, now referred to as Alternative Lengthening of Telomeres (ALT), are known to be present in various organisms and contexts[27]. Their results, however, implied that an active mechanism of *de novo* addition of sequences must exist, suggesting that there should be terminal transferase-like enzymes responsible for such event[26]. Later on, this terminal transferase-like activity was experimentally observed by newly developed assays in *Tetrahymena* protein extracts, by Greider and Blackburn[28,29]. The template behind specific-sequence polimerization at telomeres was later identified as an RNA component with a sequence complementary to the telomeric one[30]. This pointed to a mechanism of reverse-transcription for the *de novo* addition at telomeres[31,32]. The new enzyme, named telomerase[33], is composed by an RNA component (Terc) and a protein subunit (Tert) and was already described in most eukaryotes[10,34,35,36,37]. The mechanism of *de novo* addition of telomere repeats *in vivo* relies on a telomerase activity cycle of binding of the RNA component to telomere 3' overhang DNA; extension through its reverse transcriptase activity from the template; and either dissociation or translocation to repeat the cyclic polymerization. Filling of the other strand is then provided by common DNA polymerases using this template[38,39,40].

Apart from the canonical telomere-elongation function, telomerase may have non-canonical roles, controlling several cellular functions independently of telomere length changes. This can be by regulating the transcription of several genes involved in cell proliferation[41,42,43], survival (namely by controlling *wnt* and *myc* pathways)[44,45], and apoptosis[46], and hematopoietic differentiation[47]. However, this is still a controversial topic[48].

Much is now known about Tert structure and how it relates to its function and regulation in various organisms. Its structural organization can be divided into four functional domains: 1) N-terminal domain (with a conserved GQ block); Linker; 2) RNA-binding domain (with CP, QFP, and T blocks); 3) Reverse-transcriptase domain (with seven conserved RT motifs); and 3) a moderately conserved C-terminal extension. The N-terminal domain was shown to be involved in single-stranded DNA binding, and is important for the initial priming of the 3' overhang DNA at telomeres. It has an RNA-binding domain of unknown significance and is also important for enzyme processivity and activity *in vivo*. The C-terminus is highly variable and probably reflects species differences as it is dispensable for yeast enzyme activity *in vivo* but important for human and *Tetrahymena* telomerase activity. The most well studied domain, the Reverse-transcriptase one, contains seven RT motifs and a fingers-palm structure conserved with other reverse-transcriptases (as the HIV one)[38,40,49,50].

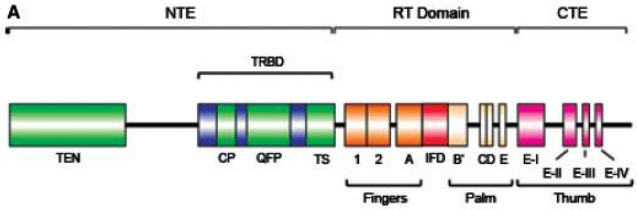

Figure 3: Schematic representation of Tert protein structure (domains and features)[40]

The role of telomerase on telomeres is highly regulated at many levels. *tert* gene transcription directly correlates with enzyme activity and several important signalling pathways impact on its expression levels. At the promoter, various components of oncogenic pathways (like the pair Myc/Mad) and growth factors act as activators and tumour suppressors (such as p53 and BRCA-1) as repressors[51]. In addition, *tert* expression levels are influenced by the chromatin status and epigenetic marks[51]. Besides this transcriptional-level regulation, telomerase holoenzyme production also involves regulated post-transcriptional events: production of splicing variants of Tert (of yet unknown significance)[50], ubiquitination and turnover of the protein[52], intracellular trafficking[53], phosphorilation and translocation to the nucleus and access to telomeres/enzymatic activity, by telomere-associated proteins[8,54].

3. The Hayflick limit, cell senescence and the cancer-ageing connexion

In the 1960s, cells were viewed as immortal as they were easily propagated in culture with appropriate media. This view changed after the work of Hayflick and others, who demonstrated that, instead, cells from a somatic tissue (human primary fibroblasts) could only divide a limited number of times in culture (the so-called *Hayflick limit*). After this, cells enter what was called Phase III or replicative cell senescence[55,56]. The immortal cells that were used for research purposes had oncogenic features, like heteroploidy or transformation by viruses, which accounted for their ability to divide indefinitely and permitted their establishment as cell lines[56]. Hayfick hypothesized that immortal cell lines can result from escaping the senescence state, through accumulation of some alterations that confer oncogenic potential[57]. This is in agreement with the fact that along with other modifications, over 90% of human cancers reactivate telomerase at some point and all of them have some kind of telomere elongating mechanism (like ALT) which accounts for their characteristic high proliferation rate[58].

The Hayflick's replicative limit is a programmed intrinsic property of cells, dependent on donor age (the limit is 50 cell divisions for embryonic-derived cultures and 20 for human adult somatic cells)[55,56]. This property was later localized in the nucleus[59,60,61] and in this

context, Olovnikov's theoretical predictions and the identification of the end-replication problem pointed to telomere shortening as the "replicometer" that counted the number of cell divisions[16,62].

Although cell senescence is well characterised, its implications *in vivo* are still an area of active investigation. Hayflick thought that replicative cell senescence was directly responsible for ageing[57]. Accordingly, one current model is that, as senescent cells accumulate in tissues, they limit the regenerative potential of stem cell pools thus conducing to failure in tissue maintenance, homeostasis and capacity to respond to physiological stress, which defines ageing[63,64]. Ageing can be seen as the consequence of failure in maintaining the active state of biomolecules due to malfunction of replacement and repair processes with time (one of them being telomere maintenance). The amount of time during which these processes can still maintain cellular functions and prevent age-associated changes account for longevity determination[65]. Therefore, in order to proceed with therapeutic approaches for slowing ageing and not just extending life with diminished health, one needs to increase both maximum longevity and median life-span (which is related to healthy live)[66].

There is a dramatic increase of cancer incidence with age, which reflects the close relationship between cancer and ageing in terms of mechanisms. A current model linking them is presented in Figure 4. Continuous division of somatic cells leads to dysfunctional telomeres and consequent arrest of proliferation, cellular senescence or cell death. Occasionally, cells escape this crisis by loss of sensors (like P53). This leads to telomere erosion and chromosomal instability. Re-activation of telomerase stabilizes telomere ends and allow for continuous tumour growth (Figure 1)[63,67,68,69].

Telomere and cell senescence implications on ageing are supported by a number of observations. Since most human somatic cells do not express telomerase[70], telomeres shorten with cell division *in vitro*[71] and *in vivo*[72]. Also, there is a strong correlation between age of cell donor/replicative capacity and initial telomere length[72]. Proliferative cell types, such as germ cells and proliferative cells in adult stem cell niches, have active telomerase and longer telomeres. However, this activity is not sufficient and telomere attrition still occurs in somatic stem cell niches with age[73,74,75,76]. Tert expression in human fibroblasts in culture allows continued cell division past the *Hayflick limit* and those cells look normal and non-oncogenic[77]. The study of telomere-associated inherited disorders, namely *dyskeratosis congenita* (DC), further supports the implication of telomere shortening in tissue degeneration. DC patients bear mutations either in the catalytic Tert component of telomerase and its regulatory subunits or in the gene for Terc, both required for the elongation of telomeres. These individuals have shortened telomeres, accelerated ageing and reduced longevity[75,78,79]. Additionally, some Ahskenazi centenarians have variations in

Tert that correlate with their longer telomeres[80]. However, a possible role of telomeres in human longevity determination still lacks experimental proof.

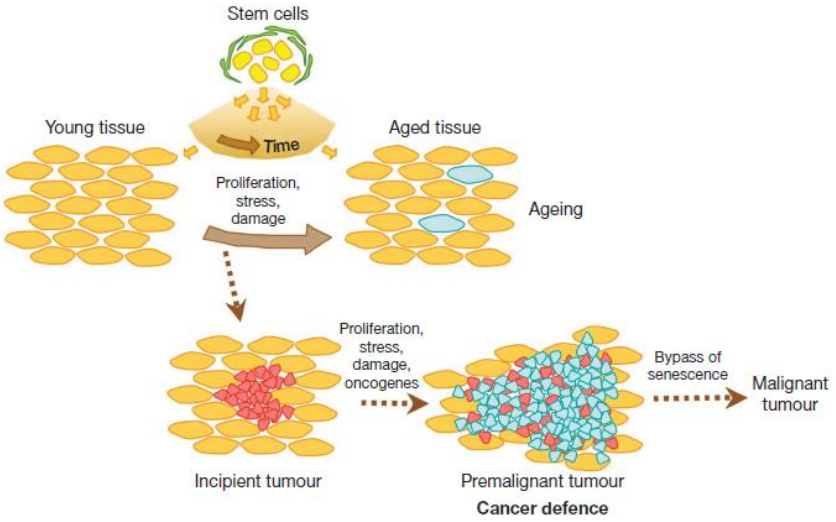

Figure 4: A model for the cancer-ageing connexion[68].

4. Mouse models for the sudy of whole organism ageing

To address these issues, mouse models were developed and extensively studied in the past years. A *knock out* model on the *Mus musculus* background was generated for the RNA component of telomerase (called mTR$^{-/-}$). These mice lack telomerase activity in all tissues and only after three generations of incrossed strains (from G1 to G6) viability and fertility diminish together with the appearance of several telomere dysfunction-associated phenotypic features. The telomere length of primary mouse embryonic fibroblasts (MEFs) decreases with population doublings as in humans and this is also coincident with phenotypic changes associated with cellular senescence[81]. Accordingly, a decrease in telomere length eventually culminates in end-to-end chromosome fusions and aneuploidy by G4[82,83]. These molecular events correlate with progressive adverse phenotypes associated with highly proliferative organs or events. Reduced fertility is explained both by defective spermatogenesis (with increased apoptosis and decreased proliferation in the testis)[84] and by decreased viability of embryos, with prevalent neural tube defects[85].

In addition to reduced body size, many ageing-associated phenotypes are also present, like brain function decline[86], hair greying and alopecia[83,87], defective hematopoiesis[84], villi architecture disruption in the gut[83,87] and higher incidence of cutaneous lesions and reduced capacity of wound healing and liver regeneration[87,88]. These phenotypes were later shown to be linked to telomere shortening in stem cell niches[42,89]. These mice also exhibit higher frequency of early-onset spontaneous malignant tumours of epithelial proliferative tissues (teratocarcinomas and skin squamous cell carcinomas), and lymphomas, which are, interestingly, more frequent in elderly humans than in old mice[87]. On

the other hand, when in the presence of carcinogens or together with mutations in several tumour suppressors[90,91], the short telomeres of these late generation *knockout* mice are protective against tumour growth, reflecting the dual role of telomerase in cancer.

However, telomeres in all *Mus musculus* strains are uncommonly long and hypervariable, ranging from 10 to 60 Kb in length[81,82,92]. Unlike what happens in humans, it is possible to detect high levels of telomerase activity in several tissues, thereby maintaining long telomeres[81], whereas lack of telomerase activity is observed in other tissues, which correlates with telomere shortening with age[82]. The above-mentioned mouse models were built on these strains. The lack of observable phenotypes in the first generation *knockout* mouse conduced to further intercrossing of $mTR^{-/-}$ mice until telomeres were made more limiting and human-like (by G4) and telomere dysfunction ensured dramatic phenotypic effects. Although murine ageing appears to have many similarities to human ageing, it seems to occur largely independently of telomere length and/or dysfunction[93]. Moreover, replicative senescence is not important to escape crisis, since ALT mechanisms are present at a much higher frequency[94]. Wild-derived strains of *Mus spretus* have an average telomere length similar to humans (8-10 Kb)[81] and have been studied as a more relevant model to human ageing and to ageing-like syndromes (like DC)[95]. Telomere shortening in these mice, both in haploinsufficiency and intact for telomerase, leads to a degenerative decline in highly regenerative organs, including the intestine (villous atrophy) and the testes (hypocellularity), and in the haematopoietic system (pancytopenia)[79,96,97].

In order to fully understand ageing and the contribution of telomere dysfunction to it, it is increasingly important to characterize other multicellular models that fill some of the caveats still left with mouse models, taking advantage of the particular properties of other organisms to directly test hypothesis for whole organism ageing.

5. Zebrafish, ageing and telomeres

Zebrafish can be a complementary model for understanding these issues. It has recently emerged as a model for ageing research[98,99,100] , along with several other fishes[101]. It exhibits gradual ageing with a longer lifespan than mouse of approximately 5 years[98,102] and is currently used for the study of age-dependent changes in various organs, such as the muscle, skeleton and the eye[103,104]. Zebrafish was also shown to display senescence-associated-biomarkers that can be consistently used for characterization and for high-throughput screenings for novel senescence-associated players[105].

Although controversial in the literature, zebrafish seem to have telomeres with the same length as humans (~15-20kb)[47] and several reports point to a role of telomere length

in ageing in teleosts[106,107,108,109]. Supporting this idea, a mutant for TRF2 presents significantly higher senescence-associated markers in comparison to *wild type* controls, and this is accompanied by central nervous system necrosis and decreased life-span[105]. *In vitro* telomerase activity can be detected in several marine species. In zebrafish, telomerase activity is low, but present, in all tissues including germ cells (with higher activity), gills, muscle, skin, gut, brain and the eyes (with lower activity)[106,109,110,111]. The Tert subunit cDNA of zebrafish telomerase was cloned and described recently[111]. *tert* mRNA is present in all tissues and the expression levels correlate with its enzymatic activity, suggesting that transcriptional regulation of the *tert* gene is a major determinant of telomerase activity in zebrafish. Tert protein is detected in the nucleus of both proliferating and post-mitotic retina cells, supporting non-canonical functions for telomerase in non-proliferative cells[111]. The same was observed in the brain, where neurogenic zones display expression of both *tert* and *terc* components although *terc* expression is more restricted with some differentiated cells expressing *tert* alone[112].

It has been proposed that this prevalent telomerase activity in fish can be related to their continuous growth and regeneration capacity[113]. Many teleosts are able to regenerate a fully functional caudal fin and this process of epimorphic regeneration involves the formation of masses of undifferentiated cells near the amputated bony fin rays, called blastemas. This highly proliferative population of cells will later on differentiate to completely restore the fin to a functional architecture[114]. Further support for this hypothesis came from the observation that telomerase activity is enhanced at 7dpa and is accompanied by telomere elongation. This up-regulation may be important for maintaining telomere length and elongate shorter telomeres during the rapid cellular proliferation required during regeneration[110]. However, a conflicting recent report claims that both ageing and regeneration are unaffected by telomerase and telomere length[115]. Previous work has shown that *knock-down* of *terc* but not *tert* leads to a smaller blastema[116]. Interestingly, in the case of *terc*, these anti-sense molecules acted as direct antagonists of the enzymatic function, resembling what is being used in clinical trials for anti-telomerase chemotherapies.

A role for telomerase on embryonic development in zebrafish was also addressed using morpholino antisense oligonucleotides against both *tert*[116,117] and *terc*[47,116] components. While *terc*-directed morpholinos caused embryonic lethality and affected brain and porterior/notochord development associated with indicators of chromosomic instability[116], *tert knock-down* only conduced to embryonic hematopoiesis impairment and resulting pancytopenia without significant changes in telomere lengths[47].

Main goals

Recently, a telomerase mutant of the *tert* subunit was generated by a N-ethyl-N-nitrosourea-*Tilling* project at the Hubrecht Laboratory at the University of Utrecht, Netherlands, identified as *tert*^{hu3430}. The initial preliminary analysis of this mutant showed already shortened telomeres in the brain of 10 months-old zygotic mutants. The loss of half the dose of telomerase activity already resulted in a decrease of telomere length which indicates that the low telomerase activity is insufficient to compensate for telomere loss during ageing and/or cell doublings in the zebrafish brain[112].

The recent observations on the importance of telomeres and/or telomerase in zebrafish, combined with several technical advantages of using zebrafish make further characterization of this mutant and the establishment of zebrafish models in this scope highly relevant for our further understanding of whole organism ageing. Furthermore, zebrafish are relatively inexpensive to maintain, they are amenable for high throughput screens, and they allow the use of sophisticated genetic and imaging tools.

Therefore, my project aimed to achieve the following goals:

- To establish genotyping techniques for the tert^{hu3430} mutant and to maintain mutant lines;
- To characterize telomere length distribution differences among genotypes;
- To assess the effects of telomerase absence and telomere status on cell proliferation-related contexts:
    - In the adult mutants, by addressing proliferative tissue maintenance with age;
    - In maternal zygotic mutant embryos, during development.

Experimental procedures

1. Zebrafish lines and husbandry

The *tert*^{hu3430} mutation (see Figure S1,Figure S2Figure S3) was generated on a *wild type* TL (tüpfel-long fin) background at the Ubrecht laboratory, Utrecht, Netherlands. Mutant lines were maintained by intercrossing heterozygous individuals and background mutations were previously removed by outcrossing three times with *wild type* (AB strain) individuals at Dr. P. Chapouton laboratory at the German Research Center for Evironmental Health, Germany. *Wild type* and heterozygous siblings were used as controls for all experiments. Maternal zygotic mutant embryos were generated by crossing adult homozygous mutant couples. The crosses between adult homozygous zygotic mutants and respective controls were performed once a week. Each couple was put together overnight on appropriate crossing boxes and the embryos were collected and maintained in embryonic media 1x (diluted with system water from a stock 50x solution: 14,69g NaCl, 0,63g KCl, 2,43g $CaCl_2.2H_2O$, 4,07g $MgSO_4.7H_2O$ – with 1mL of methylene blue/10L) which was changed daily. Embryos were staged by time post fertilization (hours, hpf, or days, dpf) at 28ºC and by morphological criteria[118]. *Wild type* AB lines were used for optimization of techniques. All fish were kept on an aquarium system at 28ºC, except when recovering from caudal fin amputation or manipulation in which they were kept in crossing boxes on a 33ºC water bath.

2. Genotyping of *tert*^{hu3430} lines

2.1. Caudal fin amputation and isolation of genomic DNA

The progenies of mutant heterozygote inter-crosses were separated after 3 months of age into breeding tanks and numbered for genotyping purposes. Each individual was separately anaesthetized with Tricaine 1x (160 mg/ml) (MS222, Sigma) and the caudal fin was amputated. The corresponding fin clip for each individual was collected into a 2mL eppendorf tube and incubated on a lysis buffer solution (Genomic DNA purification kit - #K0512, *Fermentas*) with 0,5mg/mL Proteinase K on a shaking thermomixer, overnight at 50°C. The extraction of genomic DNA was then performed as indicated on the Genomic DNA purification kit, but with the precipitation step performed overnight at -20ºC.

2.2. PCR, RFLP and sequencing

The genomic DNA was diluted in sterile nuclease-free water. After optimization, a fragment around the point mutation was amplified with proof-reading *Phusion* DNA-Polymerase (Finzymes, F-530S) and the following primers: Tert2A-1F (5'-CATCAGCACCAGCGAGGTCTGGAAG-3') and Tert2A-1R (5'-CTGTCTTCTGGACAGCAGGGGA-3') for RFLP genotyping; Tert2A-2F (5'-

GACGACCAGTTCGGATCCCTTTC-3') and Tert2A-2R (5'-CTTTACCCTCCGCCGCTTTACC-3') for genotyping by both RFLP and sequencing methods (see Figure S2). The PCR conditions were the following: 98ºC for 1min; 98ºC for 10 sec., 65ºC for 30sec., 72ºC for 1min. (for 30 cycles); and a final elongation step of 72ºC for 10min. The amplified PCR products were separated from non-incorporated nucleotides and excess primers with a Wizard® SV Gel and PCR clean-up system (Promega, #A9281). Clean PCR reactions were sequenced (StabVida, Portugal) with both the forward and reverse primers (from the Tert2A-F/R-1 or Tert2A-F/R-2 sets), separately. Additionally, the genotype of some individuals was confirmed by RFLP: the samples were subjected to digest (*Hpy188III* for 2h at 37°C - New England Biolabs) and the fragments were visualized after electrophoresis on a 3% high resolution agarose gel (MetaPhor® - FMC BioProducts, #50180 or Sigma, #A4718).

3. Telomere Restriction Fragment (TRF) Analysis

3.1. Genomic DNA isolation and digestion

Genomic DNA from adult zebrafish fins was obtained as described above for genotyping purposes. The approximate DNA concentration was measured with Nanodrop equipment (Thermo scientific, ND 1000) and the DNA was visualized on a 1% agarose gel to control DNA integrity and RNA presence (in which case 1uL of RNase A (Sigma) was added to the samples, 5 min. at 37ºC) and for relative quantification of samples for further digestion. Approximately equal amounts of DNA (~1ug) were digested with HinfI (Invitrogen or Roche) and RsaI (Invitrogen) enzymes in a total volume of 30uL at 37ºC, overnight. Control undigested samples were produced by substituting enzymes by water.

3.2. Electrophoresis and Transference

The total volume of the reaction was loaded onto a 0,6% 25cm x 15cm agarose gel in 0,5x TBE, and separated for ~17h at 110 V and 4ºC. After electrophoresis, the gel was photographed and processed for transference: after an initial step in HCl 0,25N for 15 min., it was incubated on a denaturing Blot1 solution (NaOH 0,5M; NaCl 1,5M) for 30 min. and then neutralized in Blot2 (NH_4Ac 1M; NaOH 0,02M) for 1 hour and washed with 6xSSC (NaCl 90mM; Trisodium Citrate 90mM). A 25cm x 15cm membrane (zeta-probe GT genomic tested blotting membrane, *Biorad* #162-0196) was soaked briefly on water and immersed 10min on Blot2 solution after which it was placed over 3 pieces of Blot2-embedded chromatography Whatman paper (Schleicher-Schuell, Sigma) on top of a stack of paper towels with the gel on top, wells down. The transference proceeded overnight and the DNA was crosslinked to the membrane by UV treatment (Stratalinker 1800, Stratagene).

3.3. Probe preparation, Hybridization and Detection

A telomere probe was obtained by random-primer labelling of a $(CCCTAA)_{17}$ oligonucleotide (25 ng) with the Prime-it II random primer labelling kit (Stratagene) (10uL random primers were added to the oligonucleotide in a total volume of 24uL, put in 100ºC for 5min and then 5U of Klenow enzyme in buffer were added to dCTP-αP32 (5uL from a 10mCi/ml;3000Ci/mmol stock) for 30min. at 37ºC). The non-incorporated radioactive particles were removed by filtering the resulting product on a final volume of 100uL (with TE 1x) through a Sepharose G-50 spin column (GE Healthcare). The membranes were pre-incubated for at least 30min. on the hybridization Church-Gilbert buffer (1%BSA, 1mM EDTA, 7% SDS, 0,5M $NaHPO_4$ pH 7,2) and then half the volume of the prepared probe was added to one membrane, after boiling for 5 min., and allowed to hybridize overnight at 65ºC. The membranes were washed three times with a solution of 2xSSC; 1%SDS to remove non-hybridized probe and then exposed overnight on a phosphorimager screen (GE Healthcare) The signal was detected with a Storm 860 scanner, using the GE Healthcare's ImageQuant™ software selecting for a 100 micron pixel size and phosphor-image option to obtain quantifiable 16-bit digital images.

3.4. Data Analysis of Southern Blot

Images were analysed with ImageJ 1.43u. The pixel gray values (intensity) were measured along each lane and the mean per pixel x position was recorded on xy tables (where x is the position relative to well and y is the intensity value for each point). After calibrating the x axis with the ladder bands' position, the y values were normalized to a 0-1 scale:

Formula (1) $\boldsymbol{yn = \frac{yi - ymin}{ymax - ymin}}$, with yn = normalized intensity; yi = intensity value for table position i; ymin and ymax = minimum and maximum intensity value of the well (column), respectively.

Using Matlab 7.10.0.499 (R2010a) (under the guidance of Samuel Antão, MSc, Computer Engineer), normalized data was grouped in classes, producing histograms, in order to reduce the noise influence on calculations, as described[119]. The upper and lower ranges of molecular weight corresponding to telomere signal were analysed separately. Assuming that the TRF values can be described by a normal distribution, the most likely normal function was found and divided by the molecular weight distribution in order to determine the average molecular weight (MW) value for the mean TRF frequency. Independently, the relative frequency values were calculated from experimental data by dividing the normalized intensity values by the corresponding MW, as described[119], and presented graphically. The weighted and unweighted averages were also calculated directly

from the normalized histogram intensity values by applying the formulas below, as described[120] (as in TeloRun program, by Harley,C., Allsopp, R. and Vaziri, H.):

Formula (2) Weighted mean: $\Sigma(\mathbf{ODi})/\Sigma(\mathbf{ODi/Li})$, with OD_i as the signal intensity and L_i as the DNA length at position i. It takes into account the dependency of the signal on the length of molecules and corrects for this aspect.

Formula (3) Unweighted mean: $\Sigma(\mathbf{ODi} * \mathbf{Li})/\Sigma(\mathbf{ODi})$, with OD_i as the signal intensity and L_i as the DNA length at position i.

(See supplementary materials and methods for implementation code).

4. Histological analysis

4.1. Fixation, processing and sectioning techniques

4.1.1. Fixation, processing and sectioning techniques for embryos

Embryos older than 48hpf were anaesthetised in tricaine 1x (160 mg/ml) (MS222, Sigma) in embryonic media, before fixation. All embryos were fixed overnight in 4% paraformaldeyde (PFA) at 4ºC and then placed in 100% methanol at 4ºC before processing. After several washes in PBS (phosphate buffer saline) the embryos were cryoprotected on a sucrose 15%/PBS solution and then embedded in 7,5% pork skin gelatine (Sigma)/15% sucrose/PBS for one hour at 37ºC. The $1cm^2$ blocks were frozen in isopenthane/liquid nitrogen and stored at -80ºC until sectioning. The embedded samples were cut in 12um sections with a cryostat (Leica CM 3050S) either alternately for further paired Hematoxylin-Eosin (HE) stained- and non-stained slides or serially for staining only.

4.1.2. Fixation, processing and sectioning techniques for adults

Fish were sacrificed in 25x Tricaine (MS222, Sigma) in system water and fixed overnight in 4% PFA at 4ºC. After decalcification overnight in 15% EDTA/H_2O and washes in dH_20, they were dehydrated on an ethanol series (70%, 96%, 100%) and placed on xilol. The samples were then embedded in paraffin on vacuum at 70ºC and oriented for sagittal sectioning on appropriate metallic scaffolds. The embedded samples were cut in 6um sections using a Minot microtome (Leica RM 2145). Sections were collected for further paired HE stained- and non-stained slides.

4.2. Hematoxylin-Eosin staining

4.2.1. Hematoxylin-Eosin staining for embryos

Slides were washed one hour in 1x PBS on a 37ºC water bath and then runned through a series of washing and staining steps: dH2O (5min.); Hematoxylin (5min.); dH2O

(briefly); 1% HCl (briefly); flowing H2O; NH4 (1-4 min.); 70% Ethanol (30sec.); Eosin (briefly); 70%/96%/100% Ethanol series (30sec.). The slides were mounted after application of xilol (10min.) in Entellan with 24 x 60 mm coverslips, and stored at room temperature.

4.2.2. Hematoxylin-Eosin staining for adults

Slides were deparaffinized in xilol for 15 minutes and rehydrated on a 100%/96%/70% Ethanol series (5min. each step). Then they were runned through a series of washing and staining steps: dH2O (5min.); Hematoxylin (10min.); dH2O (briefly); 1% HCl (briefly); flowing H2O; NH4 (1-4min.); 70% Ethanol (3sec.); Eosin (briefly); 70%/96%/100% Ethanol series (30sec. each). The slides were mounted with 24 x 60 mm coverslips in Entellan after application of xilol (10min.), and stored at room temperature.

5. Adult fish imaging and histology slides' image acquisition

Images from adult fish were acquired using a regular photo camera and the scale was set using a regular ruler on the image. Images from histology slides were acquired using a brightfield microscope (Leica DM2500). All images were processed with Adobe Photoshop® CS4 software and the image panels were created using Adobe Illustrator® CS4 software.

6. Embryo imaging

All images were collected with a Leica Z6 APO stereoscope with a Leica DFC 490 camera. The embryos were placed on top of a 1% agarose-coated dish in embryonic media or in Tricaine 1x (160 mg/ml) (MS222, Sigma) in embryonic media (for embryos older than ~48hpf). For one experiment of imaging of embryos below 24hpf, they were dechorionated and embedded in 3% Methyl cellulose (Sigma-Aldrich) in order to properly place them and obtain higher quality images. All images were processed with Adobe Photoshop® CS4 software and the image panels were created using Adobe Illustrator® CS4 software.

7. Statistics

The Graphpad Prism 5 program was used for statistical analysis. Comparisons between experimental and control results were made using paired a t-test with 0.95 confidence level. For $p<0.05$, differences were considered significant and the values were presented on the respective graph.

Results

1. Zebrafish *tert*^{hu3430} mutants have shorter telomeres by 6 months of age

A PCR-based assay that measures telomerase activity *in vitro* from tissue protein extracts (Telomeric Repeats Amplification Protocol – TRAP) was performed by our lab, showing that these mutant animals have no telomerase activity in several organs, therefore confirming that the nonsense mutation *tert*^{hu3430} leads to a non-functional product.

The absolute length of zebrafish telomeres is controversial in literature (see Introduction-5.). In order to determine the absolute mean telomere length of this species, we optimized the method of Telomere Restriction Fragment (TRF) analysis by Southern Blot. We used 6 months-old animals, which are still young and have already reached sexual maturity in the case of *wild types*, and caudal fin tissue because it is easily available and analysed single fins in order to account for variability.

The result obtained by this technique is a smear signal that describes the distribution of telomere length in the chromosomes of all cells within the tissue. One can then calculate the average telomere length as well as observe the distribution of lengths within each sample. Duplicate samples of three individuals from each genotype were independently digested and separated, leading to two sets of results (Figure 5).

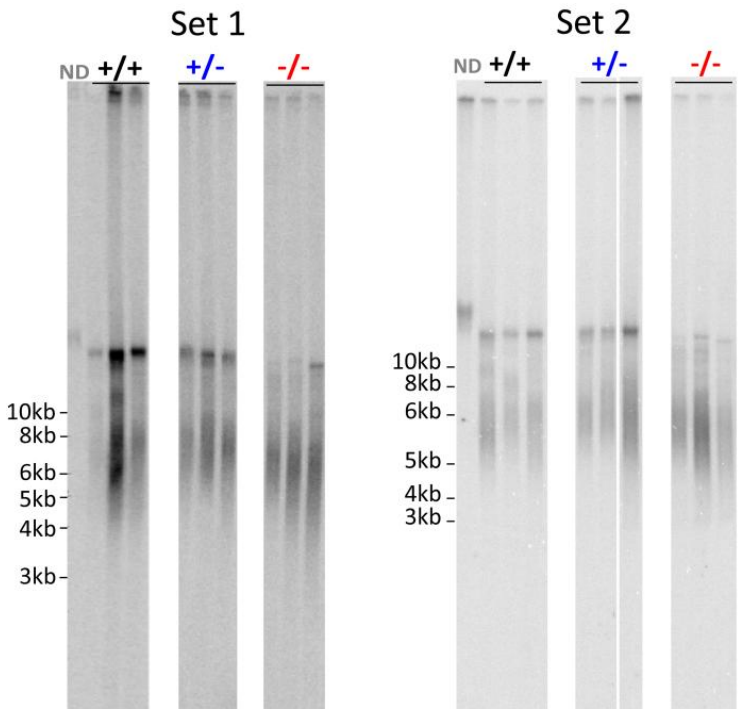

Figure 5: HinfI/RsaI TRF Southern Blot results for two duplicate sets of caudal fin samples from 6 months-old fish. Three samples per genotype were analysed in each set. Probe used: random primer-labelled $(CCCTAA)_{12}$ ^{32}P-dCTP.

Each lane was analysed in order to obtain densitometry profile data corresponding to the values of intensity on the graph varying according to the distance on the gel (Figure 6). This was then processed in order to give rise to distributions of relative frequency of TRF length for each sample (Figure 7).

As shown in Figure 5 and Figure 7, a smear from about 3 Kb to 10 Kb is present in *wild type* samples. A higher molecular weight (MW) population of TRFs of about 13,5 Kb (although the DNA ladder used does not allow for accurate measurements above 10 Kb) is also present. The overall distribution of TRFs is similar between *wild type* individuals and two populations within the lower molecular weight range are present, which can represent true distinct classes of telomere lengths in the tissue. Heterozygotes present roughly the same distribution and average telomere length as *wild types* except for the absence of the two clearly distinct populations on the lower MW range of telomeres. Homozygous mutants' samples present a TRF profile in which both higher and lower MW portions are shifted to a low MW value. Moreover, the higher MW band is compressed, suggesting that the longer molecules present in *wild types* are here shortened. The differences between genotypes are significant, as depicted in Figure 8. Mean TRF lengths are equivalent when calculated using weighted average formula (2) or by determining the best likely normal distribution (Figure 7, red line), dividing it by the MW distribution and finding its maximum (Figure 8). The shapes of the distribution of telomere lengths (Figure 6 and Figure 7) are also different between genotypes, with the homozygous mutant profiles shifted towards the left and with a sharper peak.

The results presented above indicate that, at least in this tissue, 6 months-old adult zebrafish individuals have short telomeres of about 6 to 7 Kb in average and that telomerase is important to maintain these values, since the telomerase mutants have clearly shorter telomeres with a difference of about 1 Kb in respect to *wild type* siblings. Having a clear distinction in mean telomere lengths between *wild type* and mutant siblings is particularly striking since the fin tissue is not an adult tissue with a particularly high proliferation rate (that in the absence of telomerase would be subjected to higher telomere attrition) neither these fish are particularly old (which would lead to increased telomere attrition in the absence of telomerase activity).

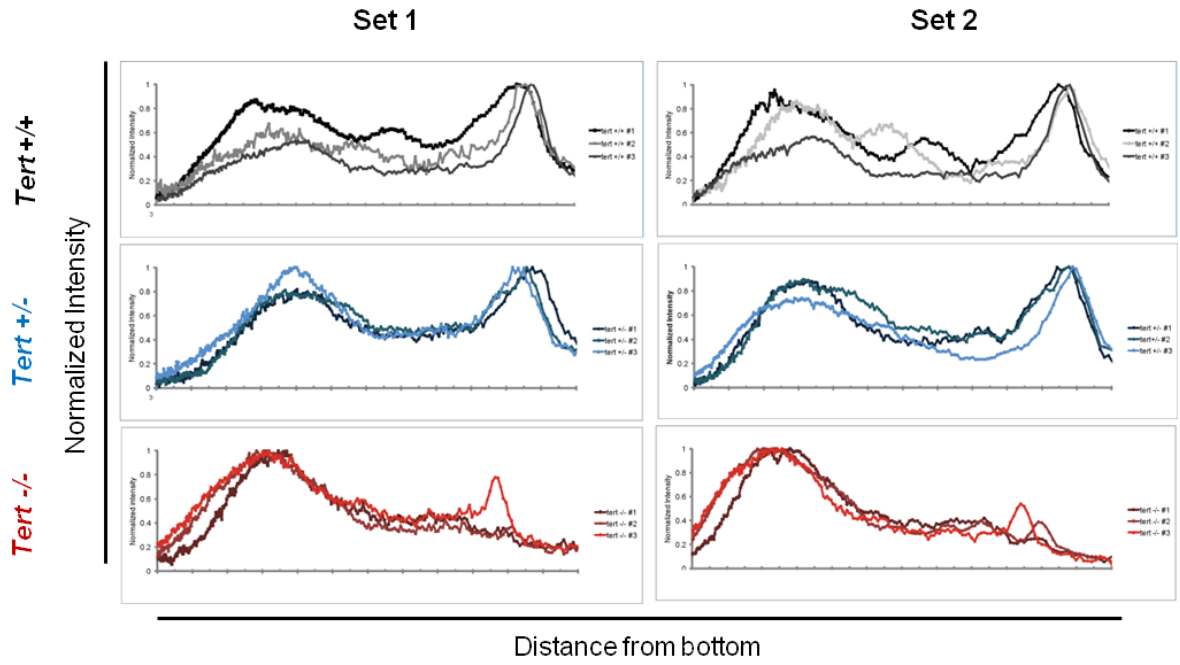

Figure 6: Densitometry graphs of intensity signals of the samples grouped by genotypes, for both sets

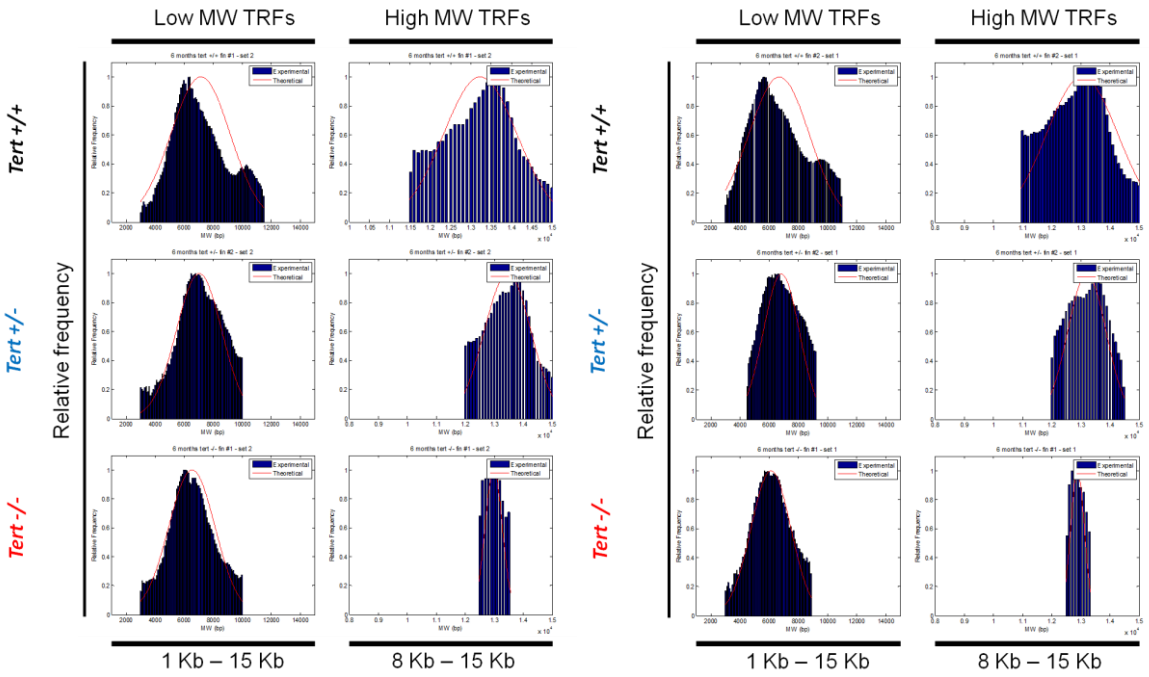

Figure 7: Relative frequency (Formula (1)) TRF length distribution of matched representative samples from each genotype from Set 1 (left) and Set 2 (right) blots.

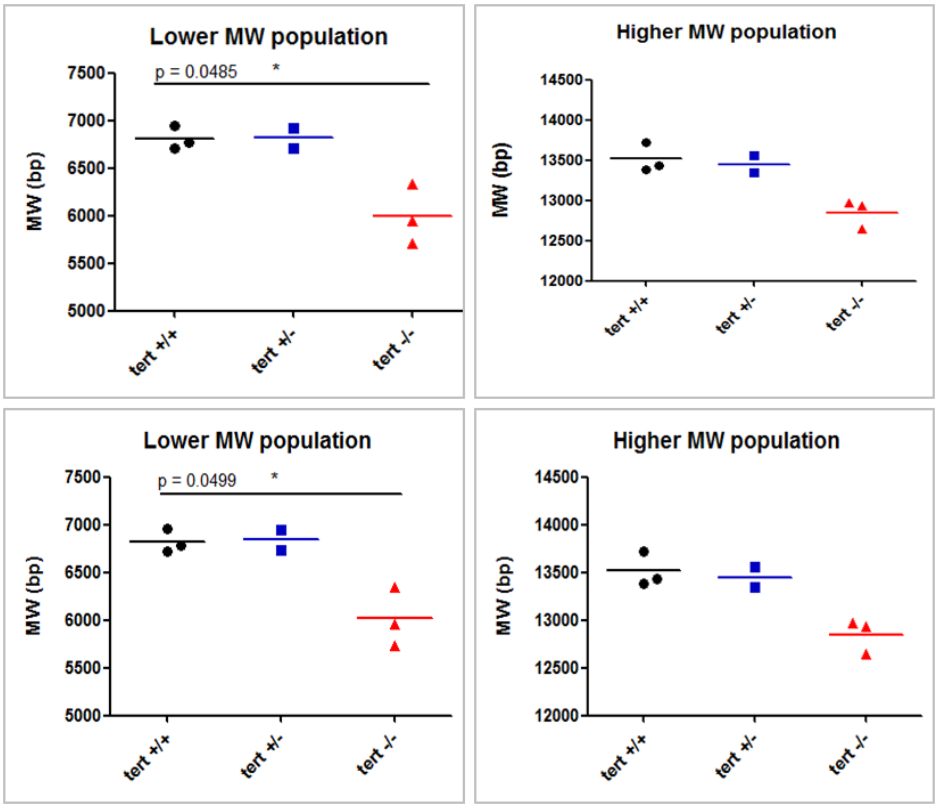

Figure 8: Average TRF length as determined with (Formula (2)) (above) or x for y maximum of a Normal distribution/MW (below). Each point is average of duplicate values for each sample. See also Figure S4 and Figure S **5**.

2. Telomerase zygotic mutants are viable but display several proliferation-related phenotypes as adults and infertility

In order to determine the effects of lack of telomerase activity in zebrafish, we followed the health status of adult zygotic mutant fish through time. Some individuals displayed progressive deterioration including altered, less bright pigmentation, diminished activity and an extreme loss of body weight. This ultimately conduced to death by one year of age. In Figure 9, we can observe the extreme thinness of these fish, which is quantified on the graph in c) in form of a width/length ratio. We were able to sacrifice one individual for subsequent analysis, whereas the others died before we could collect them in a well-preserved condition. The results of the histology analysis of this individual's tissues are presented in Figure 10 (N=1). Here we can observe that all tissues have lost their structure and integrity. They are loose, with decreased cellularity in comparison with *wild type*. The gills' branches are thinner, with just one-row of cells on gill filaments (Figure 10C/C'), the muscle fibres are disintegrated (Figure 10B/B') and the gut presents a profound atrophy of the villi with loss of intestinal crypts (Figure 10D/D'). Interestingly, the retina has an abnormal shape and a disorganized agglomerate of cells is observed instead of the characteristic layering structure (Figure 10A/A'). In the testis (Figure 10 E/E' and Eb/E'b), it is possible to observe the lack of cellularity compared with the *wild type* sample, in which mature spermatozoids are present

inside seminiferous tubules (arrows in Figure 10 Eb/E'b). These histological features are consistent with the poor health status of the individuals presented in Figure 9, although we could not conclude which was the first alteration to occur and what was their particular cause of death. Recent observations in the lab point to the testis as the first organs to show alterations, followed by the gut, since histological abnormalities in these organs are observed as soon as at 6 months of age. Although some slides were kept for subsequent immunohistochemistry, no subsequent studies were yet performed to address the telomere status of these samples *in situ* or for apoptosis. However, PCNA staining (which is a component of the DNA replication complex) performed in the lab showed that the mutant gut is devoid of proliferating cells whereas *wild type* crypts present a strong signal.

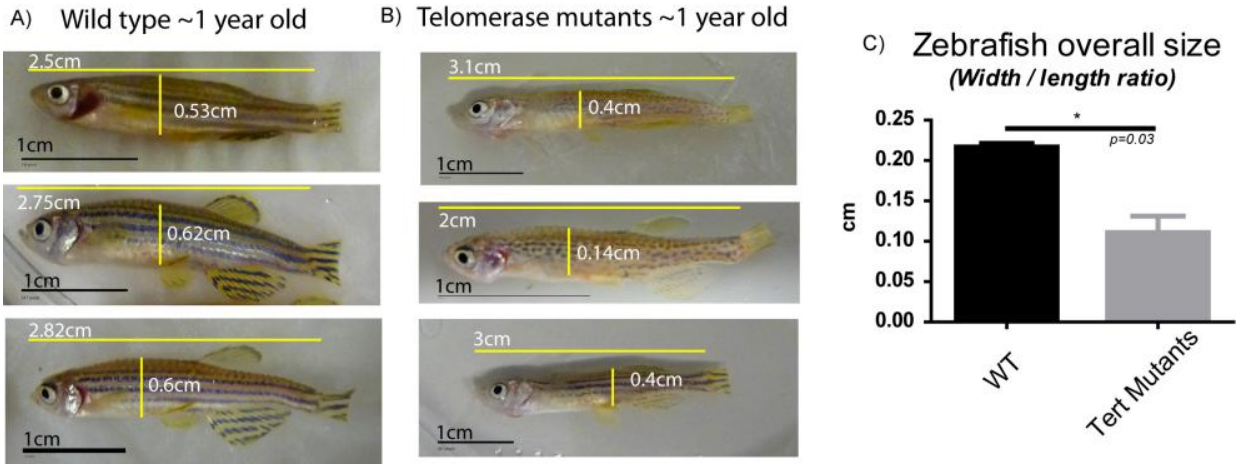

Figure 9: 1 year-old zygotic mutants displaying a 'wasting phenotype' (A) and B)) and quantification of their different width/length ratios when compared with *wild type* siblings (C)).

Both male and female homozygous mutants have also lower fertility as soon as at 6 months-old. In order to count the number of eggs and the number of viable zygotes we crossed *tert*$^{+/+}$; *tert*$^{+/-}$ and *tert*$^{-/-}$ couples. While *tert*$^{+/+}$ and *tert*$^{+/-}$ females consistently produced large amounts of eggs, the female *tert*$^{-/-}$ was only able to produce them once every two weeks (~50% of the times relative to *wild type* couple) and in lower amounts (~50%), even when coupled with *wild type* males. This progressed to a state of complete infertility at 7 months of age, and this is accompanied by severe deterioration as it was observed in the 1-year old mutants of Figure 9. Most of the eggs produced by the female *tert*$^{-/-}$ also do not appear to be fertilized by any of the *tert*$^{-/-}$ males.

To investigate whether the low fertilization index of tert-/- eggs was caused by the mutant males or females, *wild type* and homozygous mutant individuals were crossed in different combinations. As we can observe in Figure 11, most of the eggs were fertilized when the *tert*$^{-/-}$ female was crossed with a *wild type* male, similar to *wild type* incrosses. On the other hand, most of the eggs were not fertilized when *wild type* females were crossed

with the *tert*$^{-/-}$ males, similarly to what happened in the mutant couple incross. These eggs that fail to develop are similar to non-fertilized eggs from *wild type* crosses (Figure 11)..

These results point to a role of telomerase in maintaining tissue renewal in the adult. The failure in keeping tissue homeostasis compromises organism viability in the mutant and translates into infertility.

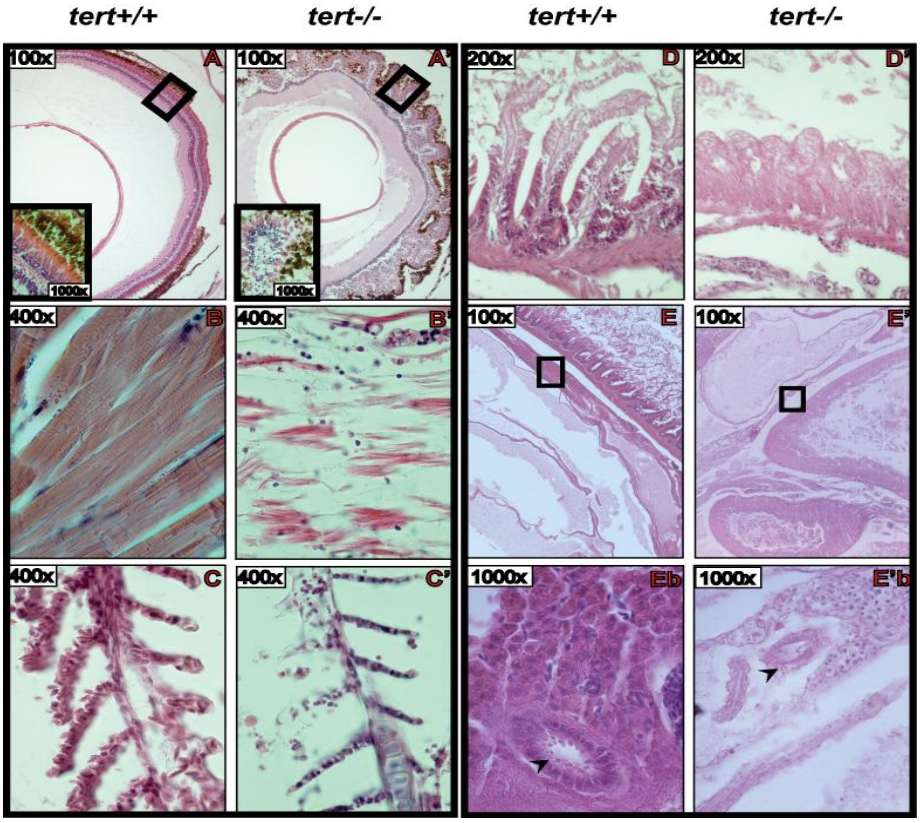

Figure 10: Microscopy images from Hematoxylin-Eosin stained sections of several tissues from adult zebrafish. Matched *wild type* (tert$^{+/+}$) and zygotic homozygous mutant (tert$^{-/-}$) samples are presented side-by-side (X: wild type; X': mutant). A and A': Retina; B and B': Skeletal muscle from trunk region; C and C': Gill filaments; D and D': Midgut wall; E and E': Visceral region showing the placement of the testis (square); Eb and Eb': Amplified image of the region on the square in E and E', respectively, showing transversal sections of seminiferous tubules (arrow).

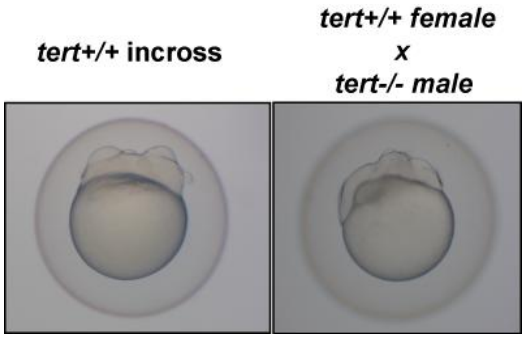

Figure 11: Phenotype of eggs resulting from a *wild type* cross (A) and from a cross between a *wild type* female and a homozygous zygotic mutant male (B).

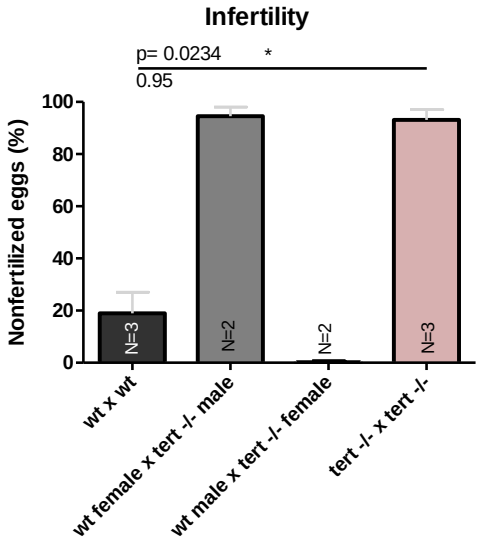

Figure 12: Percentage of non-fertilized eggs per cross (mean nr. of non-fertilized eggs/total number of eggs produced by the female). Error bars represent standard deviation interval.

3. Maternal zygotic mutants are not viable due to gross abnormalities during embryonic development

As previously mentioned, *tert*$^{-/-}$ incrosses produced a low number of zygotes due to reduced fertility of mutants (Figure 12). However, the few maternal zygotic embryos generated were raised in order to characterize their development.

All mutant embryos were unviable and presented multiple phenotypes. They were delayed in development when compared to *wild type* control embryos fertilized at the same time. This delay was detected as soon as the first cell divisions start to occur (Figure 13 A/A'). During gastrulation stages, mutant embryos showed a delay in epiboly movement, which corresponds to the movement of cell layers towards the vegetal pole of the embryo (Figure 13C' (arrows), when compared to Figure 13B'). At the end of gastrulation, the tail region of mutant embryos appears abnormal and darker, suggesting the occurrence of apoptosis (Figure 13D' (arrow)). A few hours later, during segmentation stages, the posterior region of mutants also seems to be affected when compared to *wild type* and this translates into tail malformations, which are observable at 24hpf (Figure 13Ga/G'a) and 48hpf (Figure 14C and Cb). The anterior brain region also shows defects in comparison to *wild type* (Figure 13G/G'). Interestingly, we observed that later, at 3dpf, mutant embryos' neural tube fail to close (Figure 14I and Figure 14K/K'), suggesting that *tert* has a role during brain development. The most common phenotype was a curvature of the body with associated bending of the notochord (Figure 13Ga/G'a and Figure 14C, D) and improper somite/muscle development (Figure 13E/E' and Figure 14L/L'). The posterior region anomalies were sometimes translated into severe truncations (Figure 14J). Also, even when no other striking phenotype was apparent, the eyes in the mutant were often smaller than in *wild type* (Figure 13F/F' and Figure 14 (white arrows)). In the case of one single mutant embryo that seemed

normal, it was still delayed during development and failed to inflate the swim-bladder (Figure 14G'). We also observed a reduced number of blood cells circulating near the trunk region (*data not shown*) and the heart (Figure 14B/B'), which possibly explains the high incidence of heart edemas in mutant embryos (Figure 14, black arrows). Furthermore, the pattern of distribution and the shape of mutant pigment cells (melanophores) seem to be affected in mutants in comparison to *wild type* (Figure 14C and D). Interestingly, potential apoptotic cells were observed in some of the mutant embryos, which captured the methylene blue used as a pH indicator of the embryo medium (Figure 14C, Cb and E).

This broad manifestation of telomerase absence highlights its pleiotropic role in embryonic development, which relies greatly on cellular proliferation in order to proceed normally.

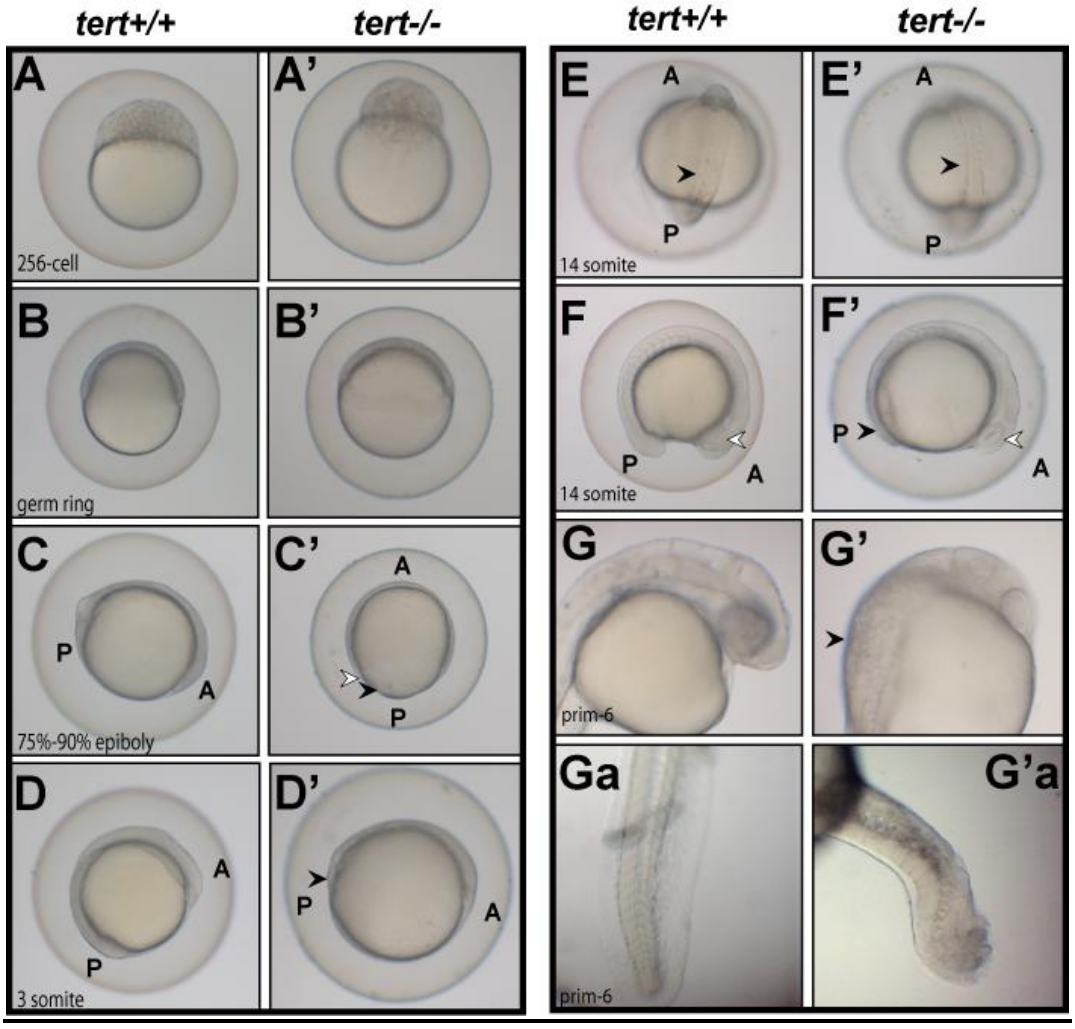

Figure 13: Time course of first hours of development of *wild type* (tert+/+) and maternal zygotic mutant (tert-/-) embryos. *Wild type* embryos were staged according to Kimmel et al., 1995 and corresponding images of mutant embryos for each time-point (A to G) is presented side-by-side. White arrow in C': EVL (enveloping layer); Black arrow in C': YSL (yolk sincitial layer); Black arrows in D' and F': embryo tail region looking abnormal; White arrow in F/F': developing eye; G and G': head region for G-corresponding time-point; Black arrow in G': particular aspect of cells near the head region, looking abnormal. Ga and G'a: tail region for G-corresponding time-point. A: Anterior; P: Posterior.

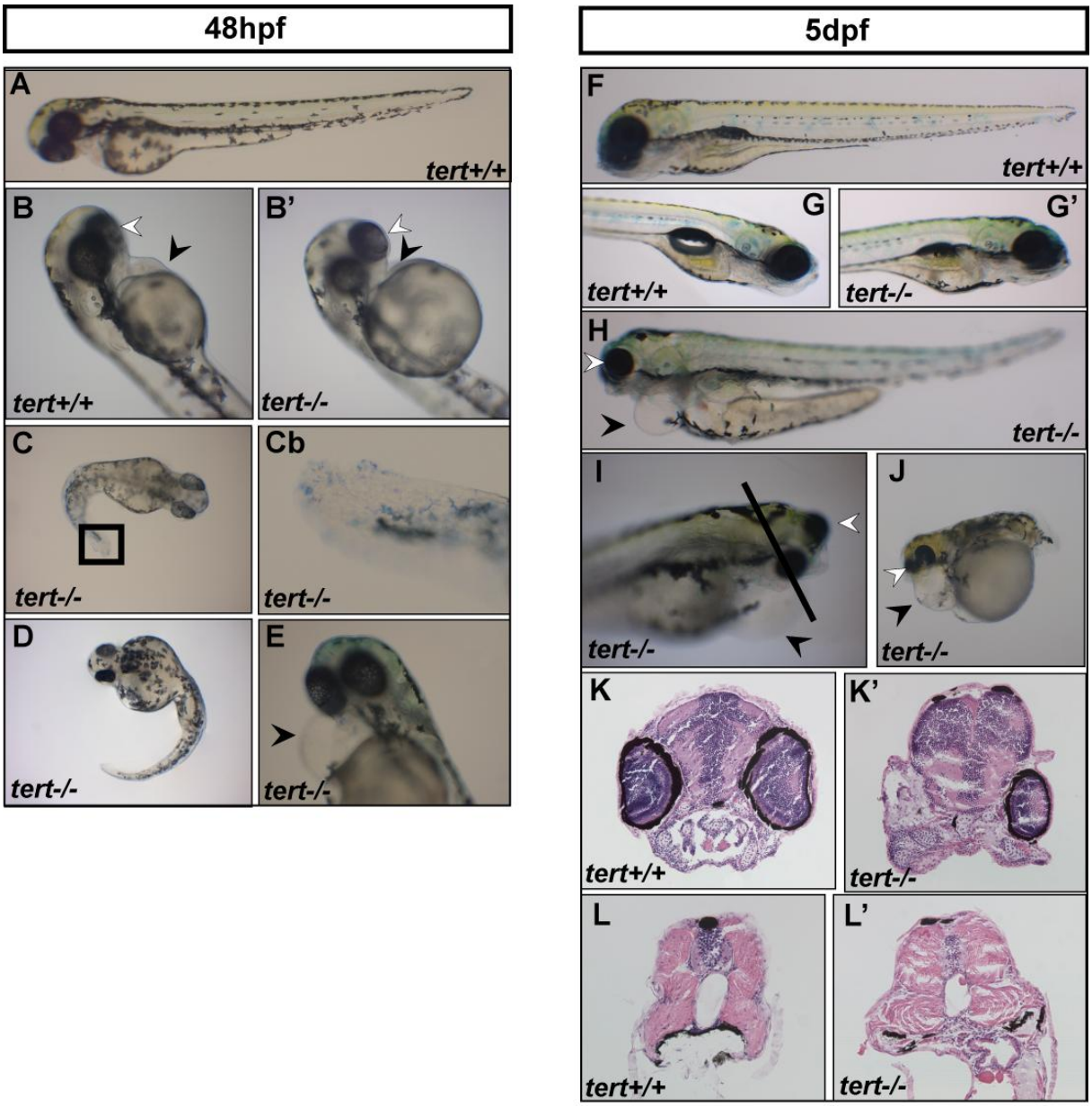

Figure 14: 48hpf (left) and 5dpf (right) - images of maternal zygotic mutants ($tert^{-/-}$) and *wild type* ($tert^{+/+}$) embryos. A: whole body image of *wild type* 48hpf embryo; B and B': anterior region, showing the eye (white arrow) and the developing heart (black arrow); C: $tert^{-/-}$ embryo showing abnormal body curvature and methylene blue- likely apoptotic stained cells; Cb: close up of square in C. D: $tert^{-/-}$ embryo showing abnormal body curvature and abnormal distribution of melanocytes; E: $tert^{-/-}$ embryo showing heart edema (arrow) and methylene blue-stained brain region. F: whole body image of *wild type* 5dpf embryo. G and G': anterior region, showing the eye, brain, and developing internal organs. H, I and J: $tert^{-/-}$ embryos, showing small eyes (white arrows) and heart edemas (black arrow). I: $tert^{-/-}$ embryo showing opened neural tube. Transversal section of the head (line) is presented in K' (K: equivalent section from *wild type*). J: $tert^{-/-}$ embryo with severe truncation. L and L': transversal section of trunk region showing decreased cellularity in the muscle in the $tert^{-/-}$ embryo (L') relatively to *wild type* (L).

Discussion

With the discovery of telomerase and the findings on the implication of telomeres in tissue maintenance and cancer, an enormous field of research on telomeres and telomerase emerged trying to uncover the intricate mechanisms behind such phenomena. How are telomeres protected from DNA repair pathways? What inhibits the action of those complexes at telomeres and how? What determines the species-specific telomere length? What determines the critically short telomere level? How are short or dysfunctional telomeres recognized and how is that signal transduced to induce cellular senescence or apoptosis? **Does telomere length and cellular senescence indeed contribute to overall ageing and does the telomere/telomerase axis determine longevity of an organism, particularly in humans?**

Most of the mouse studies performed so far were not sufficient to answer some of these questions because, unlike humans, their ageing process seems to rely very little on telomeres. Zebrafish seems to be a good alternative model for studying ageing and the role of telomeres and telomerase on cell proliferation and tissue homeostasis for organism maintenance. In this regard, zebrafish has several advantages: they are relatively inexpensive to maintain (making it possible to follow several individuals for ageing studies); they age gradually, displaying many consistent age-associated features that are similar to humans; they express senescence-associated cellular markers that allow the implementation of high-throughput screenings of ageing-related genes in embryos and of genetic and (live-) imaging tools. Furthermore, zebrafish have short telomeres of human-like length, they have low telomerase activity, and mutants for telomere-associated components lead to ageing-like phenotypes. In order to establish zebrafish as a model system to answer these questions, we first characterized a telomerase mutant.

Since there have been conflicting reports on zebrafish mean telomere length, we started by performing a TRF analysis by Southern Blot. We found that, in samples of a tissue with little proliferation (the caudal fin), zebrafish have short telomeres of about 6-7 Kb average length whereas mutants have shorter telomeres of about 5-6 Kb. Mutant individuals resulted from a heterozygote inter-cross, and therefore had a parental contribution of telomerase (mainly maternal) during embryonic development, which likely permitted their development to adulthood. These results contrast with those of other reports[47,115], which point to longer telomeres of about 20 Kb. This discrepancy might be due to incomplete digestion of the genomic DNA n the previous studies, as we observed that non-digested DNA migrates to about 20 Kb on the gel. Indeed in our experiments, we confirmed that the digestion was complete by running a non-digested sample side-by-side. Another reason for these contradictory results can be the variability among different individuals and among different

strains that have been used. To account for variability among individuals, we analysed TRF profiles from single individuals, instead of using samples from pools of genomic DNA as done in previous studies. Furthermore, we observed two different sized populations of telomeres on *wild type* samples, plus an upper TRF population of about 13,5 Kb in *wild types* and 12,5 Kb in homozygous mutants. This upper population represent most probably fragments in which the restriction enzymes didn't cut right at the level of telomere repeats but further into the subtelomeric region. Further optimization of the set of enzymes will be necessary. The low number of incrosses that this line has gone through, leading to a mixed genomic contribution from TÜ and AB strains, may explain the appearance of the two populations within the low molecular weight range. This situation highly contrasts what is observed in mice studies, in which the lines used have a high degree of inbreeding. Therefore, the zebrafish model might be closer to the human scenario than mice. We want to address this in the future, by measuring telomere lengths of different individuals and with age. Furthermore, recent studies refer to a haploinsufficiency for telomerase in maintaining telomere length in mouse and humans. It is possible that we observed a difference in mean telomere length at the first generation and in such younger individuals, in a tissue with low proliferation rate, because of progressive shortening while maintaining the lines in heterozygoty (Figure 15). Accordingly, we observed some difference in the TRF distribution between *wild types* and heterozygotes (the absence of the two telomere populations in heterozygotes). Further more controlled experiments will be performed in the future to address this hypothesis, as it has been done in the mouse[79].

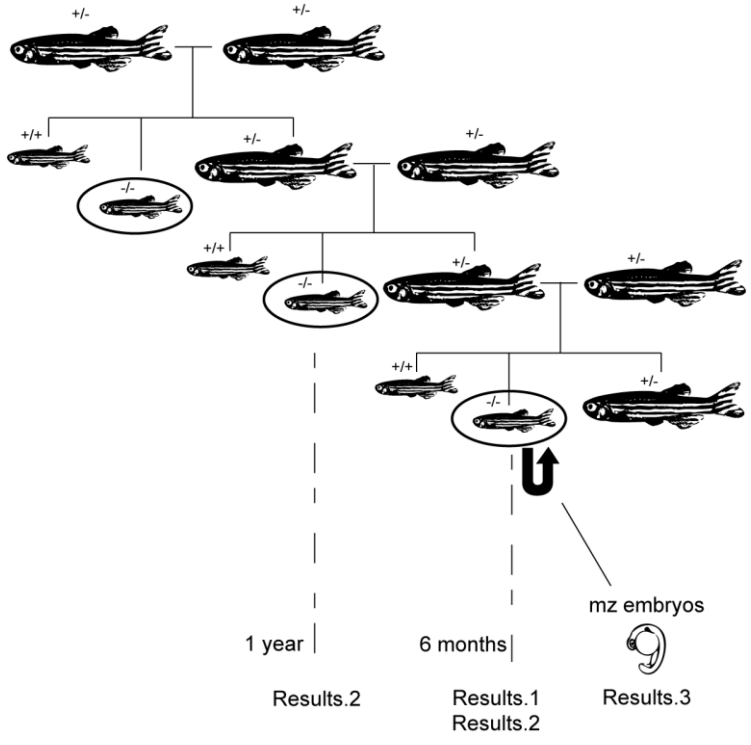

Figure 15: crosses scheme and lines used for experiments

Zebrafish age-related features are: spinal curvature related with muscle degeneration, a *wasting* phenotype with loss of body weight and gut function impairment, cataracts, retinal atrophy and with drusen-like lesions (similar to what happens in macular degeneration), cholinergic-dependent cognitive performance decline and alterations in sleep, increased incidence of several pathological lesions and decline in reproductive and regenerative capacity. This is accompanied by an accumulation of senescence markers, namely senescence-associated β-galactosidase (SA-β-gal) in skin and muscle, oxidized proteins in muscle and lipofuscin granules in the liver (as in mice and humans)[103].

We have shown that telomerase deficiency leads to progressive organ degeneration which, at 1 year of age, conduces to an overall loss of body weight and culminates in precocious death (see Results-2.). Moreover, males have reduced fertility by 6 months of age, producing few progeny, which can be explained by the testis atrophy observed in 1-year-old mutants (see Results-2.). The few fertilized embryos resulting from a *tert*$^{-/-}$ incross exhibit development defects consistent with lack of cellular proliferation or increased apoptosis (see Results-3.).

The earlier reduction in body weight and decrease in viability is typical of aged fish and was also observed in the mouse mTR$^{-/-}$ model, although just after G3, and it was accompanied by gut villi architecture disruption as we observe in our mutant fish[83]. The gut epithelia undergoes frequent renewal, which requires extensive cell proliferation. Although we were not yet able to measure telomere length in other tissues than the caudal fin, it is possible that this conduced to telomere loss and growth impairment (as suggested by the lack of PCNA staining in homozygous mutant intestinal crypts), senescence or apoptosis of the epithelial cells. Many of the anomalies we found by histological examination of homozygous mutants and the observed infertility may be explained following the same rationale and these phenotypes are highly similar to what has been observed in the mouse and also in human age-associated diseases (See Introduction-4.). Interestingly, we have not found an increase in the incidence of neoplasia on proliferative tissues as it was observed in the mTR$^{-/-}$ mouse (see Introduction-4.). Although chromosomic instability may be present, the absence of telomerase in zebrafish mutants would prevent further growth of tumour cells. In mice, this growth may be supported by ALT mechanisms[121]. We can therefore speculate that in zebrafish telomerase is the main mechanism for telomere elongation in cancer progression, as it is in humans (see Introduction-3.).

To further investigate the cause of these phenotypes, it will be crucial to make an overall assessment of telomere length in different organs and of individuals of various ages, by comparing naturally ageing *wild types* with both heterozygous (as referred earlier) and homozygous mutants, and then by relating that to telomerase activity levels in those organs.

Furthermore, it will be important to perform other techniques apart from TRF analysis by Southern Blot in order to quantify telomere length differences *in situ*, using Q-FISH and Telomapping[89,122]. These techniques allow the detection of critically short telomeres, which are the actual triggers of the DNA damage response at telomeres. We would like to link this information with further characterization of the phenotypes by assessing cellular senescence (by SA-β-gal staining), cell proliferation index (using mitotic, P-H3, and S-phase, PCNA, markers), apoptosis (by TUNEL assay and immuno-histochemistry against cleaved caspase-3), genomic instability (together with Q-FISH, one can observe fusions and karyotipic abnormalities in metaphase spreads) and DNA damage at telomeres (combining Q-FISH with immuno-cytochemistry against the γH2AX histone variant).

Perhaps the most important result was that homozygous mutant embryos coming from a homozygous mutant incross did not survive, unlike what happen in the mouse, where 4 to 6 generations were needed to observe diminished viability of the offspring, mainly due to failure to close the neural tube[85]. From these results, it is possible that our experimental set-up is sufficient to lead to the one short/dysfunctional telomere that alone can trigger a DNA damage response and lead to cell cycle arrest, senescence or apoptosis, and halt embryonic development. The high requirement for maternal contribution during embryonic development in zebrafish may also account for this premature phenotype in comparison to mouse studies.

All the maternal zygotic mutants were unviable and displayed gross abnormalities in a wide spectrum of phenotypes (see Results-3.). During zebrafish embryonic development, the *tert* subunit is expressed broadly during the initial stages (until tailbud stage), becomes further restricted to the head and tail regions (4-10 somite stages), and is later particularly located in the central nervous system and the eyes[112]. The expression of the *terc* component is broader, but also stronger, in the brain, eyes, tail[112,116]and trunk[116], at later stages. The phenotypes we observed are consistent with these expression patterns, namely delayed development during initial stages, eyes of reduced size, failure to close the neural tube (as it happens in the mouse), body curvature possibly due to problems in muscle development, and apoptotic-like cells in the head and tail (see Results-3.). Defects in the head, tail and trunk (namely our most frequent phenotype, embryo trunk curvature), associated with chromosomic instability, were also observed previously by using morpholinos against *terc*[116]. However, previous work using morpholinos against *tert* did not reveal any striking phenotype apart from defects in hematopoiesis (see Introduction-5.)[47,116]. Maybe *knock-down* or the fact that there are two splicing variants of *tert* in zebrafish, at the terminal region, still allows for the presence of Tert protein. We also observed reduced number of blood cells in circulation (*data not shown*) and in the heart, which likely conduced to heart edema at later stages (See Results-3.). In order to characterize further these phenotypes, it

would be interesting to perform *in situ* hybridyzation for muscle and brain development genes and proliferation-related genes like *myc*. We also plan to cross our mutant line with a recently developed transgenic line that allows the visualization of cell cycle progression in the embryo *in vivo*[123]. Additionally, as in the adult, it will be crucial to directly link telomere dysfunction to these phenotypes with the use of telomere-measurement techniques *in situ*, the observation of karyotypes and the use of several molecular markers to detect apoptosis, problems in cell cycle progression, senescence and DNA damage. Importantly, a previous report[47] describes no difference in telomere length when *knocking-down tert* expression, leding the authors to propose that the observed phenotypes are related to non-canonical functions of telomerase. Further studies will be required to clarify the role of telomerase in such a highly proliferative event as is embryonic development.

Final remarks

The results on the initial characterization of the *tert*^{hu3430} mutant, here presented, are promising for the establishment of zebrafish as a model for telomere biology research. Zebrafish do have short telomeres and telomeres of homozygous mutants are significantly shorter, strongly indicating that telomerase is a fundamental mechanism for telomere maintenance in this organism. The phenotypes of the mutant are consistent with a role of telomerase in cell proliferation and tissue maintenance in the adult, namely impaired organ renewal and function, which leads to a decline in the health status and precocious death by 1 year of age. Infertility arises as one of the first consequences of telomerase absence, which reflects the high proliferation rate required for gonad function and the high telomerase activity levels present in wild type zebrafish. A role for telomerase on cell proliferation is also evident on the developmental defects of maternal zygotic mutant embryos that make them unviable.

In the future, after further characterizing the mutant, our laboratory will test if telomeres and telomerase are actually determinants of longevity. To accomplish that, we will follow mutants and *wild types* in an extremely controlled set-up and telomerase will be conditionally expressed temporally. With this, we intend to answer whether ageing is a no-return process and if not which are the stages and organs in which therapeutics would be fruitful. Zebrafish has also been used as a model for cancer and telomerase is known to have an important role in cancer appearance and progression. In this regard, we mean to use zebrafish to directly model anti-telomerase therapeutics and to determine which stage will benefit from this approach. Our lab is also interested in further characterizing the role of telomerase in regeneration, which is a process that relies greatly on cell proliferation.

Bibliography

1 McClintock, B. (1941) The Stability of Broken Ends of Chromosomes in *Zea Mays*. *Genetics*. **26**(2)**:** 234-282.
2 Greider, C.W. (1996) Telomere length regulation. *Ann. Rev. of Biochem.* **65**(1)**:** 337–365.
3 Ferreira, M.G., Miller, K.M., Cooper, J.P. (2004) Indecent Exposure: When Telomeres Become Uncapped. *Mol. Cell.* **13**: 7-18.
4 DeBoeck, G., Forsyth, R.G., Praet, M., Hogendoorn, P.C. (2009) Telomere-associated proteins: cross-talk between telomere maintenance and telomere-lengthening mechanisms. *J. Pathol.* **217**: 327-344.
5 Denchi, E.L. (2009) Give me a break: how telomeres suppress the DNA damage response. *DNA repair.* **8**(9)**:** 1118-1126.
6 Subramanian, L., Nakamura, T.M. (2010) To fuse or not to fuse: how do checkpoint and DNA repair proteins maintain telomeres? *Frontiers in bioscience*.**15**(1)**:** 1105-1118.
7 Giraud-Panis, M-J., Pisano, S., Poulet, A., Le Du, M-H., Gilson, E. (2010) Structural identity of telomeric complexes. *FEBS letters*. **584**(17)**:** 3785-3799.
8 Shore, D., Bianchi, A. (2009) Telomere length regulation: coupling DNA end processing to feedback regulation of telomerase.
9 Schoeftner, S., Blasco, M.A. (2010) Chromatin regulation and non-coding RNAs at mammalian telomeres. *Seminars in cell & developmental biology*. **21**(2)**:** 186-193
10 Gomes, N.M.V., Shay, J.W., Wright, W.E. (2010) Telomere biology in Metazoa. *FEBS letters.* (July) [Epub ahead of print].
11 Azzalin, C.M., Epub ahead of print].Reichenbach, P., Khoriauli, L., Giulotto, E., Lingner, J. (2007) Telomeric repeat containing RNA and RNA surveillance factors at mammalian chromosome ends. *Science.* **318**(5851)**:** 798-801.
12 Isken, O., Maquat, L.E. (2009) Telomeric RNAs as a novel player in telomeric integrity. *F1000 Biol. Rep.* **1**:90.
13 Luke, B., Lingner, J. (2009) TERRA: telomeric repeat-containing RNA. *The EMBO J.* **28**(17)**:** 2503-2510.
14 Feuerhahn, S., Iglesias, N., Panza, A., Porro, A., Lingner, J. (2010) TERRA biogenesis, turnover and implications for function. *FEBS letters.* (July) [Epub ahead of print].
15 Schoeftner, S., Blasco, M.A. (2009) A 'higher order' of telomere regulation: telomere heterochromatin and telomeric RNAs. *The EMBO J.* **28**(16)**:** 2323-2336.
16 Olovnikov, A. (1973) A theory of marginotomy: the incomplete copying of template margin in enzymic synthesis of polynucleotides and biological significance of the phenomenon. *J. Theoret. Biol.* **41**(1):181-190.
17 Watson, J.D. (1972) Origin of concatameric T7 DNA. *Nature New Biology.* **239:** 197-201.
18 Huffman, K.E., Levene, S.D., Tesmer, V.M., Shay, J.W., Wright, W.E. (2000) Telomere shortening is proportional to the size of the G-rich telomeric 3'-overhang. *J. of Biol. Chem.* **275**(26)**:** 19719-19722.
19 Lundblad, V., Szostak, J.W. (1989) A mutant with a defect in telomere elongation leads to senescence in yeast. *Cell.* **57**(4)**:** 633-643.
20 Longhese, M.P., Bonetti, D., Manfrini, N., Clerici, M. (2010) Mechanisms and regulation of DNA end resection. *The EMBO J.* **29**(17)**:** 2864-2874.
21 Pitt, C.W., Cooper, J.P. (2010) Pot1 inactivation leads to rampant telomere resection and loss in one cell cycle. *Nucleic Acids Research.* (July) [Epub ahead of print].
22 Levy, M.Z., Allsopp, R.C., Futcher, A.B., Greider, C.W., Harley, C.B. (1992) Telomere End-replication Problem and Cell Aging. *J. Mol. Biol.* **225:** 951-960.
23 Palm, W., deLange, T. (2008) How shelterin protects mammalian telomeres. *Ann. Rev. of Gen.* **42:** 301-34.
24 Greider, C.W. (2010) Telomerase Discovery: The Excitement of Putting Together Pieces of the Puzzle (Nobel Lecture). *Angewandte Chemie (International ed. in English)*. **21205:** 7422-7439.
25 Szostak, J.W., Blackburn, E.H. (1982) Cloning yeast telomeres on linear plasmid vectors. *Cell*. **29**(1)**:** 245–255.
26 Shampay, J., Szostak, J.W., Blackburn, E.H. (1984) DNA sequences of telomeres maintained in yeast. *Nature.* **310:** 154-157.
27 Cesare, A.J., Reddel, R.R. (2010) Alternative lengthening of telomeres: models, mechanisms and implications. *Nature Rev. Genet.* **11**(5)**:** 319-330.
28 Greider, C.W., Blackburn, E.H. (1985) Identification of a specific telomere terminal transferase activity in *Tetrahymena* extracts. *Cell*. **43:** 405-413.
29 Greider, C.W., Blackburn, E.H. (1987) The telomere terminal transferase of *Tetrahymena* is a ribonucleoprotein enzyme with two kinds of primer specificity. *Cell*. **51**(6)**:** 887-898.
30 Greider, C.W., Blackburn, E.H. (1989) A telomeric sequence in the RNA of *Tetrahymena* telomerase required for telomere repeat synthesis. *Nature*. **337**(6205)**:** 331–337.
31 Greider, C.W. (1991) Telomerase is processive. *Mol. and Cell. Biol.* **11**(9)**:** 4572-4580.
32 Harrington, L.A., Greider, C.W. (1991) Telomerase primer specificity and chromosome healing. *Nature*. **353:** 451-454.
33 Collins, K., Kobayashi, R., Greider, C.W. (1995) Purification of *Tetrahymena* telomerase and cloning of genes encoding the two protein components of the enzyme. *Cell.* **81**(5)**:** 677-686.
34 Nakamura, T.M., Morin, G.B., Chapman, K.B., Weinrich, S.L., Andrews, W.H., Lingner, J., Harley, C.B., Cech, T.R. (1997) Telomerase Catalytic Subunit Homologs from Fission Yeast and Human. *Science*. **277:** 955-959.
35 Prowse, K.R., Avilion, A.A., Greider, C.W. (1993) Identification of a nonprocessive telomerase activity from mouse cells. *PNAS.* **90**(4)**:** 1493-147.
36 Lingner, J., Cech, T.R. (1996) Purification of telomerase from *Euplotes aediculatus*: requirement of a primer 3' overhang. *PNAS.* **93**(20)**:**10712-10717.
37 Watson, J. M., Riha, K. (2010) Comparative biology of telomeres: Where plants stand. *FEBS letters*. **584**(17)**:** 3752-3759.
38 Kelleher, C., Teixeira, M.T., Förstemann, K., Lingner, J. (2002) Telomerase: biochemical considerations for enzyme and substrate. *Trends in Biochem. Sciences*. **27**(11)**:** 572-579.
39 Osterhage, J.L., Friedman, K.L. (2009) Chromosome end maintenance by telomerase. *J. Biol. Chem.* **284**(24)**:** 16061-16065.
40 Wyatt, H.D.M., West, S.C., Beattie, T.L. (2010) InTERTpreting telomerase structure and function. *Nucleic Acids Res.* **38**(17)**:**5609-5622
41 Smith, L.L., Coller, H.A., Roberts, J.M. (2003) Telomerase modulates expression of growth-controlling genes and enhances cell proliferation. *Nature cell biology.* **5**(5)**:** 474-479.
42 Flores, I., Cayuela, M.L., Blasco, M.A. (2005) Effects of telomerase and telomere length on epidermal stem cell behavior. *Science.* **309:** 1253-1256.
43 Sarin, K.Y., Cheung, P., Gilison, D., Lee, E., Tennen, R.I., Wang, E., Artandi, M.K., Oro, A.E., Artandi, S.E. (2005) Conditional telomerase induction causes proliferation of hair follicle stem cells. *Nature.* **436**(7053)**:** 1048-1052.

44 Choi, J., Southworth, L.K., Sarin, K.Y., Venteicher, A.S. , Ma, W., Chang, W., Cheung, P., Jun, S., Artandi, M.K., Shah, N., KimS.K., Artandi, S.E. (2008) TERT promotes epithelial proliferation through transcriptional control of a Myc- and Wnt-related developmental program. *PLoS genetics.* **4**(1)**:** 124-138.
45 Park, J-I., Venteicher, A.S, Hong, J.Y., Choi, J., Jun, S., Shkreli, M., Chang, W., Meng, Z., Cheung, P., Ji, H., McLaughlin, M., Veenstra, T.D., Nusse, R., McCrea, P.D., Artandi, S.E. (2009) Telomerase modulates Wnt signalling by association with target gene chromatin. *Nature*. **460:** 66-72.
46 Lu, C., Fu, W., Mattson, M.P. (2001) Telomerase protects developing neurons against DNA damage-induced cell death. *Dev. Brain Res.* **131:** 167-171.
47 Imamura, S., Uchiyama, J., Koshimizu, E., Hanai, J-I., Raftopoulou, C., Murphey, R:D., Bayliss, P.E., Imai, Y., Burns, C.E., Masutomi, K., Gagos, S., Zon, L.I., Roberts, T.M., Kishi, S. (2008) A non-canonical function of zebrafish telomerase reverse transcriptase is required for developmental hematopoiesis. *PloS one.* **3**(10)**:** e3364.
48 Vidal-Cardenas, S.L., Greider, C.W. (2010) Comparing effects of mTR and mTERT deletion on gene expression and DNA damage response: a critical examination of telomere length maintenance-independent roles of telomerase. *Nucleic Acids Research*. **38**(1)**:** 60-71.
49 Autexier, C., Lue, N.F. (2006) The Structure and Function of Telomerase Reverse Transcriptase. *Annu. Rev. Biochem*. **75:**493–517.
50 Sýkorová, E., Fajkus, J. (2009) Structure–function relationships in telomerase genes. *Biology of the Cell.* **101**(7)**:** 375-392.
51 Kyo, S., Takakura, M., Fujiwara, T., Inoue, M. (2008) Understanding and exploiting hTERT promoter regulation for diagnosis and treatment of human cancers. *Cancer science.* **99**(8)**:** 1528-1538.
52 Oh, W., Lee, E-W., Lee, D., Yang, M-R., Ko, A., Yoon, C-H., Lee, H-W., Bae, Y-S., Choi, C.Y., Song, J. (2010) Hdm2 negatively regulates telomerase activity by functioning as an E3 ligase of hTERT. *Oncogene*. **29**(28)**:** 4101-4112.
53 Gallardo, F., Chartrand, P. (2008) Telomerase biogenesis: The long road before getting to the end. *RNA biology.* **5**(4)**:** 212-215.
54 Stern, J.L., Bryan, T.M. (2008) Telomerase recruitment to telomeres. *Cytog. Genome Res.* **122:** 243-54.
55 Hayflick, L., Moorhead, P.S. (1961) The serial cultivation of human diploid cell strains. *Exp. Cell Res.* **25:** 585-621.
56 Hayflick, L. (1965) The limited in vitro lifetime of human diploid cell strains." *Exp. Cell Res.* **37:** 614-636.
57 Hayflick, L. (1970) Aging under glass. *Mutation Research.* **256:** 69-80.
58 Harley, C.B. (2008) Telomerase and cancer therapeutics. *Nature Rev. Cancer*. **8**(3)**:** 167-79.
59 Wright, W.E., Hayflick, L. (1975) Nuclear control of cellular aging demonstrated by hybridization of anucleate and whole cultured normal human fibroblasts. *Exp. Cell Res.* **96:** 113-121.
60 Hayflick, L. (1976) Cellular aging studied by the reconstruction of replicating cells from nuclei and cytoplasms isolated from normal human diploid cells. *Exp. Cell Res.* **103:** 321-330.
61 Hayflick, L. (1984) Intracellular determinants of cell aging. *Cell.* **28:** 177-185.
62 Hayflick, L. (1998) How and why we age. *Exp. Gerontol.* **33**(98)**:** 639 - 653.
63 Collado, M., Blasco, M.A., Serrano, M. (2007) Cellular senescence in cancer and aging. *Cell*. **130**(2)**:** 223-233.
64 Sharpless, N.E., DePinho, R. (2004) Telomeres, stem cells, senescence, and cancer. *J. Clinical Inv.* **113**(2)**:** 160-168.
65 Hayflick, L. (2007) Entropy explains aging, genetic determinism explains longevity, and undefined terminology explains misunderstanding both. *PLoS genetics*. **3**(12)**:** e220.
66 Austad, S. (2010) Recent advances in vertebrate aging research 2009. *Aging cell.* **9**(3)**:** 297-303.
67 Serrano, M., Blasco, M.A. (2007) Cancer and ageing: convergent and divergent mechanisms. *Nature Rev. Mol. Cell Biol.* **8**(9)**:** 715–721.
68 Finkel, T., Serrano, M., Blasco, M.A. (2007) The common biology of cancer and ageing. *Nature Rev*. **448:** 767-774.
69 Artandi, S.E., DePinho, R.A. (2000) A critical role for telomeres in suppressing and facilitating carcinogenesis. *Curr. Op.Gen. & Dev.* **10**(1)**:** 39-46.
70 Forsyth, N.R., Wright, W.E., Shay, J.W. (2002) Telomerase and differentiation in multicellular organisms: turn it off, turn it on, and turn it off again. *Differentiation; research in biological diversity*. **69:** 188-97.
71 Harley, C.B., Futcher, A.B., Greider, C.W. (1990) Telomeres shorten during ageing of human fibroblasts. *Nature*. 345: 458-460.
72 Allsopp, R.C., Vaziri, H., Patterson, C., Goldstein, S., Younglai, E.V., Futcher, A.B., Greider, C.W., Harley, C.B. (1992) Telomere length predicts replicative capacity of human fibroblasts. *PNAS.* **89**(21): 10114-10118.
73 deLange, T., Shiue, L., Myers, R.M., Cox, D.R., Naylor, S.L., Killery, A.M., Varmus, H.E. (1990) Structure and variability of human chromosome ends. *Mol. Cell Biol.* **10**(2)**:** 518-527.
74 Flores, I., Canela, A., Vera, E., Tejera, A., Cotsarelis, G., Blasco, M.A. (2008) The longest telomeres: a general signature of adult stem cell compartments. *Genes & Dev.* **22**(5)**:** 654-667.
75 Sahin, E., Depinho, R.A. (2010) Linking functional decline of telomeres, mitochondria and stem cells during ageing. *Nature*. **464:** 520-528.
76 Flores, I., Benetti, R., Blasco, M.A. (2006) Telomerase regulation and stem cell behaviour. *Curr. Op.Cell Biol.* **18**(3)**:** 254–260.
77 Bodnar, A.G., Ouellette, M., Frolkis, M., Holt, S.E., Chiu, C.P., Morin, G.B., Harley, C.B., Shay, J.W., Lichtsteiner, S., Wright, W.E. (1998) Extension of life-span by introduction of telomerase into normal human cells. *Science*. **279:** 349-352.
78 Armanios, M. (2009) Syndromes of Telomere Shortening. *Ann. Rev. Genomics and Human Genet.* **10:**45-61.
79 Armanios, M., Alder, J.K., Parry, E.M., Karim, B., Strong, M.A., Greider, C.W. (2009) Short telomeres are sufficient to cause the degenerative defects associated with aging. *Am.J. Human Genet.* **85**(6)**:** 823-832.
80 Atzmon, G., Cho, M., Cawthon, R.M., Budagov, T., Katz, M., Yang, X., Siegel, G., Bergman, A., Huffman, D.M., Schechter, C.B., Wright, W.E., Shay, J.W., Barzilai, N., Govindaraju, D.R., Suh, Y. (2010) Genetic variation in human telomerase is associated with telomere length in Ashkenazi centenarians. *PNAS*. **107**(S1)**:** 1710-1717.
81 Prowse, K.R., Greider, C.W. (1995) Developmental and tissue-specific regulation of mouse telomerase and telomere length. *PNAS.* **92:** 4818-4822.
82 Blasco, M.A., Lee, H.W., Hande, M.P., Samper, E., Lansdorp, P.M., DePinho, R.A., Greider, C.W. (1997) Telomere shortening and tumor formation by mouse cells lacking telomerase RNA. *Cell.* **91:** 25-34.
83 Herrera, E., Samper, E., Martin-caballero, J., Flores, J.M., Lee, H.W., Blasco, M.A. (1999) Disease states associated with telomerase deficiency appear earlier in mice with short telomeres. *The EMBO J.* **18:** 2950-2960.
84 Lee, H.W., Blasco, M.A., Gottlieb, G.J., Horner, J.W., Greider, C.W., DePinho, R.A. (1998) Essential role of mouse telomerase in highly proliferative organs. *Nature*. **392:** 569-574.
85 Herrera, E., Samper, E., Blasco, M.A. (1999) Telomere shortening in mTR-/- embryos is associated with failure to close the neural tube. *The EMBO J.* **18**(5)**:** 1172-1181.

86 Lee, J., Jo, Y.S., Sung, Y.H., Hwang, I.H., Kim, H., Kim, S-Y., Yi, S.S., Choi, J-S., Sun, W., Seong, J.K., Lee, H-W. (2010) Telomerase Deficiency Affects Normal Brain Functions in Mice. *Neurochem. Res*. **35**(2)**:**211-218.
87 Rudolph, K.L., Chang, S., Lee, H.W., Blasco, M.A., Gottlieb, G.J., Greider, C.W., DePinho, R.A. (1999) Longevity, stress response, and cancer in aging telomerase-deficient mice. *Cell.* **96:** 701-712.
88 Rudolph, K. L. Chang, S., Millard, M., Schreiber-Agus, N., DePinho, R.A. (2000) Inhibition of Experimental Liver Cirrhosis in Mice by Telomerase Gene Delivery. *Science*. **287:** 1253-1258.
89 Flores, I., Canela, A., Vera, E., Tejera, A., Cotsarelis, G., Blasco, M.A. (2008) "The longest telomeres: a general signature of adult stem cell compartments. *Genes & Dev.* **22**(5)**:** 654-667.
90 Greenberg, R.A., Femino, A., Gottlieb, G.J., Greider, C.W., Chin, L., Lee, K.H., Singer, R.H., DePinho, R.A. (1999) Short dysfunctional telomeres impair tumorigenesis in the INK4a (delta2/3) cancer-prone mouse. *Cell*.**97:**515-525
91 Blasco, M.A. (2005) Mice with bad ends: mouse models for the study of telomeres and telomerase in cancer and aging. *The EMBO J.* **24**(6)**:** 1095-1103.
92 Zijlmans, J.M., Martens, U.M., Poon, S.S., Raap, A.K., Tanke, H.J., Ward, R.K., Lansdorp, P.M.. (1997) Telomeres in the mouse have large inter-chromosomal variations in the number of T2AG3 repeats. *PNAS.* **94:** 7423-7428.
93 Sharpless, N.E., DePinho, R.A: (2007) How stem cells age and why this makes us grow old. *Nature Rev.Mol. Cell Biol.* **8**(9)**:** 703-713.
94 Wright, W.E., Shay, J.W. (2000) Telomere dynamics in cancer progression and prevention: fundamental differences in human and mouse telomere biology. *Nature Medicine*. **6**(8)**:** 849-851.
95 Armanios, M., Chen, J-L, Chang, Y-P.C., Brodsky, R.A., Hawkins, A., Griffin, C.A., Eshleman, J.R. Cohen, A.R., Chakravarti, A., Hamosh, A., Greider, C.W. (2005) Haploinsufficiency of telomerase reverse transcriptase leads to anticipation in autosomal dominant dyskeratosis congenita. *PNAS.* **102**(44)**:** 15960-4.
96 Coviello-McLaughlin, G.M., Prowse, K.R. (1997) Telomere length regulation during postnatal development and ageing in *Mus spretus*. *Nucleic Acids Res.* **25**(15)**:** 3051-3058.
97 Hao, L-Y., Armanios, M., Strong, M.A., Karim, B., Huso, D., Greider, C.W. (2005) Short telomeres, even in the presence of telomerase, limit tissue renewal capacity. *Cell.* **123**(6)**:** 1121-1131.
98 Kishi, S. (2003) The zebrafish as a vertebrate model of functional aging and very gradual senescence. *Exp. Gerontol.* **38**(7)**:** 777-786.
99 Keller, E.T., Murtha, J.M. (2004) The use of mature zebrafish (*Danio rerio*) as a model for human aging and disease. *CBP*. **138**(3)**:** 335-341.
100 Gerhard, G.S, Cheng, K.C. (2002) A call to fins! Zebrafish as a gerontological model. *Aging Cell*. **1**(2)**:** 104-111.
101 Gerhard, G.S. (2007) "Small laboratory fish as models for aging research." *Ageing Res. Rev*. **6:** 64-72.
102 Gerhard, G.S., Kauffman, E.J., Wang, X., Stewart, R., Moore, J.L., Kasales, C.J., Demidenko, E., Cheng, K.C.. (2002) Life spans and senescent phenotypes in two strains of Zebrafish (*Danio rerio*). *Exp.Gerontol.* **37:** 1055-1068.
103 Kishi, S., Slack, B.E., Uchiyama, J., Zhdanova, I.V. (2009) Zebrafish as a genetic model in biological and behavioral gerontology: where development meets aging in vertebrates-a mini-review. *Gerontology.* **55**(4)**:** 430-41.
104 Yu, L., Tucci, V., Kishi, S., Zhdanova, I.V. (2006) Cognitive aging in zebrafish. *PloS one.* **1:** e14.
105 Kishi, S., Bayliss, P.E., Uchiyama, J., Koshimizu, E., Qi, J., Imamura, S., Islam, A., Neuberg, D., Amsterdam, A., Roberts, T.M. (2008) The Identification of Zebrafish Mutants Showing Alterations in Senescence-Associated Biomarkers. *PLoS Genetics*. **4**(8): e1000152.
106 Au, D.W.T., Mok, H.O.L., Elmore, L.W., Holt, S.E. (2009) "Japanese medaka: a new vertebrate model for studying telomere and telomerase biology. *CBP*. **149**(2)**:** 161-167.
107 Hatakeyama, H., Nakamura, K-I., Izumiyama-Shimomura, N., Ishii, A., Tsuchida, S., Takubo, K., Ishikawa, N. (2008) The teleost *Oryzias latipes* shows telomere shortening with age despite considerable telomerase activity throughout life. *Mech. of ageing and dev.* **129**(9)**:** 550-557.
108 Hartmann, N., Reichwald, K., Lechel, A., Graf, M., Kirschner, J., Dorn, A., Terzibasi, E., Wellner, J., Platzer, M., Rudolph, K.L., Cellerino, A., Englert, C. (2009) Telomeres shorten while Tert expression increases during ageing of the short-lived fish *Nothobranchius furzeri*. *Mech. of ageing and dev.* **130**(5)**:** 290-296.
109 McChesney, P.A., Elmore, L.W., Holt, S.E. (2005) Vertebrate marine species as model systems for studying telomeres and telomerase. *Zebrafish*. **1**(4)**:** 349-355.
110 Elmore, L.W., Norris, M.W., Sircar, S., Taylor Bright, A., McChesney, P.A., Winn, R.N., Holt, S. (2008) "Upregulation of telomerase function during tissue regeneration. *Exp. Biology and Medicine.* **233**(8): 958-967.
111 Lau, B.W., Wong, A.O., Tsao, G.S., So, K.F., Yip, H.K. (2008) Molecular cloning and characterization of the zebrafish (*Danio rerio*) telomerase catalytic subunit (telomerase reverse transcriptase, TERT). *J. Mol. Neurosci.* **34**: 63-75.
112 Sprungala, S. (2009) Telomere length, telomerase and maintenance of stem cells in the adult zebrafish brain. *PhD dissert. Technischen Universität München*. pp. 1-173.
113 McChesney, P.A., Elmore, L.W., Holt, S.E. (2005) Vertebrate marine species as model systems for studying telomeres and telomerase. *Zebrafish*. **1**(4)**:** 349-355.
114 Tal, T.L., Franzosa, J.A., Tanguay, R.L. (2009) Molecular Signaling Networks That Choreograph Epimorphic Fin Regeneration in Zebrafish - A Mini-Review. *Gerontology*. 56(2):231-240.
115 Lund, T.C., Glass, T.J., Tolar, J., Blazar, B.R. (2009) Expression of Telomerase and Telomere Length Are Unaffected by either Age or Limb Regeneration in *Danio rerio*. *PLoS ONE*. **4**(11)**:** e7688.
116 Mateus, R.D. (2008) Regeneração da Barbatana Caudal em Peixe-Zebra (*Danio rerio*): Papel da Telomerase. *Dissertação de Mestrado. Universidade de Lisboa*, pp. 1-30.
117 Imamura, S., Uchiyama, J., Koshimizu, E., Hanai, J-I., Raftopoulou, C., Murphey, R:D., Bayliss, P.E., Imai, Y., Burns, C.E., Masutomi, K., Gagos, S., Zon, L.I., Roberts, T.M., Kishi, S. (2008) A non-canonical function of zebrafish telomerase reverse transcriptase is required for developmental hematopoiesis. *PloS one.* **3**(10)**:** e3364
118 Kimmel, C.B., Ballard, W.W., Kimmel, S.R., Ullmann, B, Schilling, T.F. (1995) Stages of embryonic development of the zebrafish. *American Journal of Anatomy*. **203**(3)**:** 253–310.
119 Herbert, B.S., Shay, J.W., Wright, W.E. (2003) Analysis of telomeres and telomerase. *In* Methods in molecular biology. Morgan, K. (ed.). Wiley (New York). pp. 18.6.1-18.6.20.
120 Kimura, M., Stone, R.C., Hunt, S.C., Skurnick, J. , Lu, X., Harley, C.B., (2010) Measurement of telomere length by the Southern blot analysis of terminal restriction fragment lengths. *Nature Protocols*. **5**(9)**:** 1596-1907.
121 Foley, J.E., Yeh, J-R.L., Maeder, M.L., Reyon, D., et al. (2009) Rapid mutation of endogenous zebrafish genes using zinc finger nucleases made by Oligomerized Pool ENgineering (OPEN). *PloS one*. **4**(2)**:** e4348.
122 Benetti, R., García-Cao, M., Blasco, M.A. (2007) "Telomere length regulates the epigenetic status of mammalian telomeres and subtelomeres. *Nature genetics.* **39**(2)**:** 243-250

123 Canela, A., Vera, E., Klatt, P., Blasco, M.A. (2007) High-throughput telomere length quantification by FISH and its application to human population studies. *PNAS.* **104:** 5300-5305.
124 Sugiyama, M., Sakaue-Sawano, A., Iimura, T., Fukami, K. Kitaguchic, T., Kawakamie, K., Okamotof, K., Higashijimag, S., Miyawakia, A. (2009) Illuminating cell-cycle progression in the developing zebrafish embryo. *PNAS.* **106**(49)**:** 20812-7.

Annexes

Supplementary Materials and Methods

Example of MATLAB Program code used for TRF analysis:

```
clear all

close all

clc
%%%open our experimental data%%
fid = fopen('name of table data','r');

%%%data is a matrix of 10 columns%%%
dados = fscanf(fid,'%f %f %f %f %f %f %f %f %f %f',[10 inf]);
fclose('all');

%%%Define range to analyse, i.e., define low and high background position (row on
the table)%%%
rg1 = 'row number':1:'row number';
range = rg1;

%%%define which is the sample to analyse (column)%%%
x = dados(1,range);
y = dados(10,range);

%%%This is to group the data into histograms. One has to integrate data to find the
most likely column number value%%%
%return a value from the experimental, if the x is not in the experimental
%data, an interpolation is performed
exp_inter = @(aaa) interp1(x,y,aaa,'linear');

%define bars:
first_bar = 12000;   %value of MW for the first bar
bar_range = 100;    %range covered by one bar

%create bars
k1 = 0;
while (first_bar+bar_range*k1) < max(x)
    bar_x(k1+1) = first_bar+bar_range*k1;
    bar_y(k1+1) = 0;
    k1 = k1 +1;
end

num_bars = k1;

%get the value for the first bar

if num_bars == 0 %we have no bars
    return;
end

if num_bars == 1 %there is only one bar (no practical interest)
    bar_y(1) = quad(exp_inter,min(x),max(x));
    bar_x(1) = (min(x) + max(x))/2;
end

if num_bars > 1 %there are at least 2 bars
    bar_y(1)        = quad(exp_inter,min(x),bar_x(1)+bar_range/2);
    bar_x(1)        = (min(x) + bar_x(1)+bar_range/2)/2;

    bar_y(num_bars) = quad(exp_inter,bar_x(num_bars)-bar_range/2,max(x));
    bar_x(num_bars) = (bar_x(num_bars)- bar_range/2 + max(x))/2;

    for k1 = 2:(num_bars-1)
```

```
        bar_y(k1) = quad(exp_inter,bar_x(k1)-bar_range/2,bar_x(k1)+bar_range/2);
    end
end

%%%Fit the most likely normal distribution for the data, at 95% confidence level%%%
data = bar_x;
frequencies = bar_y;
confidence_level = 0.95;
censoring = zeros(size(data)); %no censoring

[mu,sigma,confidente_int_mu,confidence_int_sigma]=normfit(data,1-
confidence_level,censoring,frequencies);

%find the scale factor that result in smaller r^2
%theoretical values
scale_x = bar_x;
scale_y = normpdf(scale_x,mu,sigma);

%experimental mean
experimental_mu = ones(size(bar_y)).* mean(bar_y);

%function that compute r^2 for different scales
r2_value = @(scale) -1 + sum((bar_y - (scale_y.*scale)).^2)/ sum((bar_y -
experimental_mu).^2);

[scale, scaleval] = fminsearch(r2_value, 100);

r2 = -scaleval;

%compute scaled distribution
plot_x = min(x): 0.01: max(x);
plot_y = normpdf(plot_x,mu,sigma) .* scale;

%%%Plot the resulting histograms and the Gaussian distribution also%%%
figure
bar(bar_x,(bar_y./bar_x)./max(bar_y./bar_x));
hold on
plot(plot_x,(plot_y./plot_x)./max(plot_y./plot_x),'r-');
title ('6 months tert -/- fin #3 - set 2');%example
xlabel('MW (bp)');
ylabel('Relative Frequency');
legend('Experimental','Theoretical');
axis([8000 15000 0 1.1]);
print('-dmeta','graph_s4mut3_high.emf');

%%%Calculate the x value corresponding to maximum for the already calculated Gauss
function over x (MW) function,
%%%which is the average telomere length%%%
[maxy,maxx] = max(plot_y./plot_x);
maxx = plot_x(maxx);

%%%calculate mean trf from experimental data directly%%%

weighted_average = sum(bar_y)/sum(bar_y./bar_x)
unweighted_average = sum(bar_y.*bar_x)/sum(bar_y)
```

Supplementary Figures

Figure S1: Schematic overview of the tert^{hu3430} mutation. A T to A point mutation at the second exon of the gene that corresponds to the end of the protein N-terminus shall lead to a truncated non-functional protein. Sequencing chromatograms show the point mutation following the CGTG underlined sequence.

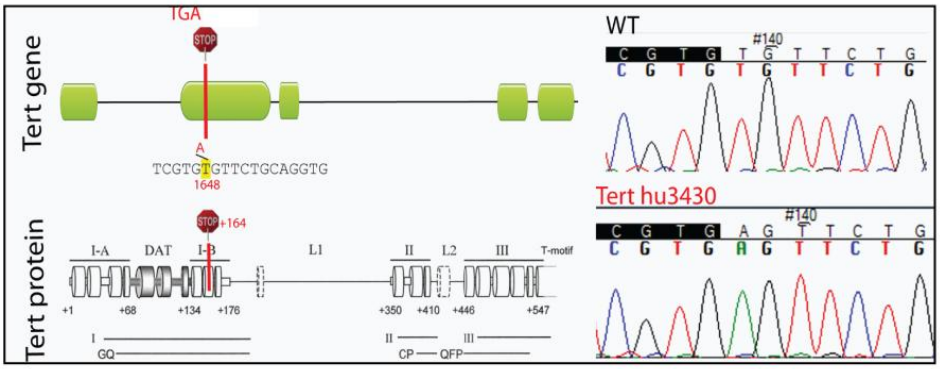

Figure S2: Part of the *wild type ztert* gene sequence corresponding to the mutation site. Exons are underlined in blue. Tert2A-F1 and Tert2A-R1-corresponding sequences are in red. Tert2A-F2 and Tert2A-R2- corresponding sequences are in green (a mismatch between primers and DNA sequence is evidenced in grey). The Mutation site is in yellow (the mutation changes T to A). The place of *Hpy188III* recognition for RFLP is signalled.

ztert gene Exons 1 and 2

>ref|NW_001880283.1|DrUn_WGA3234_3:81072-96023 Danio rerio genomic contig, reference assembly (based on Zv7_NA757)

ATGGCGGATTCAGGCCGGT
TTTGGAGATTCTGCGCTCCTTATATCCAGTCGTGCAGACTTTGGAGGAGTTCACCGACGGACTGCAATTC
CCTGACGGCCGAAAGCCGGTTCTGCTGGAGGAAACAGACGGCGCGCGCTTTAAAAAGCTCCTCAGTGGAC
TTATTGTATGCGCCTACACGCCGCCGCAGCTGCGCGTCCCCGCCCAGGTACAGTTGATTTGTTTACAATT
TATCGATCACTTAATTTAAGTGAGCTCTGTCATTGATTATAATAACTTTTGAGTCTGCTGCTGTGCGTGT
TTCTGTCACATGTCTGAAGCTCTCCTCATGTTTCATAATTATAGAACCAGATCAAGTAACCAAAGCACTG
CCGCTGATAGTGTTTCTAACACAGTGTAACGTTACACTTCCTAGTCTTGTTTTATTTTAGAAAATAAATA
TTTTACAGTCTATATTAAAGAAATTTGATTGATTTAATCACGTTAAAGGTAAATGAATCAAACGTGCGAA
AAATACTAATATAACCACATTAAAAAAACACTATAGTAATTTAAAGTAATACTGTTGTGTGTTTTAACCC
TACTATGGTAAAGTATTTGAATTAAACTGTTGTGGTGATTCTACAGTAAACAAACACTGTGGTCATGTGT
TTTATTTTACTACAGTACACCAAAGTTTACTGTAGTAAAAGTACAAGTGTATACTACTGTATTTATTAGT
TTATCAGATGATACTGTGCTGTATTGTAAATATTGTAATATATACAATATAATACACTTTACTTAAGTAT
TTGTATGTGGTGAGCAGCACATCTGTTTGAACACTGTTTGGTCAAAAATATACAGCATAAGTTTAACATG
TTTATTTGCCAGCAGTGCTTTCCTTCAACAATATTCCGGGAATTCCATTATGCTGGTTAGTAATGGTTTT
TAAAAATGAAACCTAAAAAGAATCTTAAATAAGATTATTTAATTCCAAAACAGCCGAAGAGAAGCCAATT
TATTTACTATAAAACTCACCTGCTTGATTGTTTATTATGTTGCGACATTGTAAAAATCGACATGATTTTG
TTGAAGGCTTTTTTGAAATACATAACAAAAATGTTATGCAAATAAAATCAACTTAATAGTTAATTTAGTG
TTAACCAGGAATTTTTTTTTACCGTAGCAGTTTACTATATATATATATTTTTTAATCAATTTTCATCATT
ACTGCCCTACTAAACATTGCACATCCATAACTGAGTTACGGCCAATGTTCTTCTATGTTTTCAGGATTTA
AAAATATTTATGTATGTTTTTCTCTACAAATAAAAGAAATGTGTGTTATTTCAGCTCAGCACCCTGCCGG
AGGTCTTGGCGTTCACTCTGAACCACATTAAACGTAAGAAACTGAGGAACGTCCTGGGCTTCGGTTATCA
ATGCAGCGACGTGACGACCAGTTCGGATCCCTTCCGTTTCCATGGTGACGTTTCGCAGACGGCTGCTTCC
ATCAGCACCAGCGAGGTCTGGAAGCGTATCAACCAGCGTCTGGGCACGGAGGTAACGCGGTACCTGCTGC
A Hpy188III
AGGACTGTGCCGTTTTCACCACCGTCCCGCCATCGTGTGTTCTGCAGGTGTGCGGAGAACCTGTTTACGA
CTTGCTGATGCCGCGCTCATGGTCTGGCTTTTTCCTCAGTAACTCAGATAATGAACGAATCAGCGGCGCG
ATGCGGAAATCCCCTGCTGTCCAGAAGACAGTCGCAATTTCCAAAAAGAGAACAAGAGATAACGAAAAAT
ATATTTCGGTAAAGCGGCGGAGGGTAAAGGAAACTGTGAATAATAATAACGGAAATTACAGATCTCGGTG
TTTTGCAATTTCTAAAAAGAGAGCGAGAGATAATGAAGAAAATATTTCGTTAAAGCGACGGAGGATGGAG
GAAACTGACCAAGAAGCGAAAATACGTAATGAAAATCACGGATCTCAGAGTTTCACAATTTCTAAAAAGA
GAGCGAGAGATAACGAAGAAAATATTTCGTTAAAGCGACAAAGGATGGAGGAAATTGACCAAGTAGCGAA
AATACGTAACGAAAATCACGGATCTCAGAGTTGGAAACCAGCGGATCAGCGTCCTCCTCGACCCTCGCAA
TGTTCAATACGCGTTCTGAGCATGCTCTACAATGGGCGGGGCATGAAGAACTTCCTGCTCAACAGGAAGT
TGAAAGGAGTGGGCGGGGCCAGGCGCATGCAAGGGGAGGATCTTGTCCGCATGATTTTCCTCCAATCAGA
ATCCAACGATAGCAAACCGAAAAAACTTCCTAAACGATTCTTCGCAATGGTGCCGCTATTCAGTCGGCTG
TTGCGGCAGCACAGGAAGTGTCCGTATCGGCTGTTCCTGCAAAGAAAGTGTGCAGGAAATCCAGACGTGG
AGGATATGGAGTCTCTGCTGAAGTCACACTCGTCTCCATATAGAGTTTATCTGTTCGTCAGGGAGTGTCT
GCGCCATATTATTCCCCACGAGCTCTGGGGCTGCCAGGAAAACCAGCTCCACTTCCTGTCTAATGTAAAG
AACTTCCTGCTTCTGGGGAAGTTTGAGCGCCTCACGCTGGTCCAGCTGATGTGGAGGATGAAGGTTCAGG
CCTGCCATTGGCTGGGGCCCAAGAAACGTGAGTGTGTGTGTGTGCTTTAAATGTGTGTATGTTCATATA
TATATATATATATATATATGAGTGTGTGTGTGTGCTTCTGCAGGTCAGTGTGCGAGCGAGCACCGCTA
CCGTGAGTGGATGTTGGGTCAGTGTATGGGCTGGGTGTTGAGTGGTTTTGTGGTCGGTCTGGTCAGAGCT

Figure S3: *Wild type* zTert protein sequence. The Mutation site is in yellow (the mutation changes Cysteine (C) to a STOP codon signal).

zTERT protein a.a sequence

>tr|B6ZLJ8|B6ZLJ8_DANRE Telomerase reverse transcriptase OS=Danio rerio GN=tert PE=2 SV=1

MSGQYSTDGGFRPVLEILRSLYPVVQTLEEFTDGLQFPDGRKPVLLEETDGARFKKLLSG
LIVCAYTPPQLRVPAQLSTLPEVLAFTLNHIKRKKLRNVLGFGYQCSDVTTSSDPFRFHG
DVSQTAASISTSEVWKRINQRLGTEVTRYLLQDCAVFTTVPPSCVLQVCGEPVYDLLMPR
SWSGFFLSNSDNERISGAMRKFPAVQKTVAISKKRTRDNEKYISVKRRRVKETVNNNNGN
YRSLCFAISKKRAIDNEENISLKRRRMEETDQVAKIRNENHESQSFAISKKRARDNEENI
SLKRQRMEEIDQVAKIRNENHGSQSWKPADQRPPRPSQCSIRVLSMLYNGRGMKNFLLNR
KLKGVGGARRMQGEDLVRMIFLQSESNDSKPKKLPKRFFAMVPLFSRLLRQHRKCPYRLF
LQRKCAGNPDVKDMESLLKSHSSPYRVYLFVRECLRHIIPHELWGCQENQLHFLSNVKNF
LLLGKFERLTLVQLMWRMKVQACHWLGPKKRQCASEHRYREWMLGQCMGWMLSGFVVGLV
RAQFYITESMGHKHTLRFYRGDVWSRLQDQAFRAHLCKGQWRPLSPSQALKVPNSAVTSR
IRFIPKTSSMRPITRLSGSRDTLQYFQSCVRVLQNVLSVCVREAPGPMGSTVWGWQDIHR
RLQDFSPQQKSSPRPLYFVKVDVSGAYDSLPHLKLVEVLKEVLGPFAEQSFFLRQYSSVW
SDPTRGLRKRFCTKAEMSEPLNMKGFVVDEQVSGRLHDAILVERHSSEVRGGDVFQFFQK
MLCSYVIHYDQQMFRQVCGIPQGSSVSSLLCNLCYGHMEKALLKDIAKGGCLMRLIDDFL
LITPHLSKATEFLTTLLSGVPDYGCQINPQKVAVNFPVCVSWVNSGVSVLPSSCLFPWCG
LMIHTHTLDVYKDYSRYDGLSLRYSLTLGSAHSPSTVMKKLLSVLSIKSTDIFLDLRLNS
VEAVYRSLYKLILLQALKFHACVRSLPLGQSVNRNPSFFLKMIWRMTRVTNKLLTHINKG
LPVCSVDSGGVLQSEAVQLLFCLAFETLFRRFRSVYHCLIPALHKRKRALQRELCGITLA
RVRQASSPRIPLDFSMRV

START site

Mutation site

TRF analysis

Set 1 - low MW range

name	range	bar range	confidence level	υ	conf interval υ	σ	conf interval σ	x for y max from Gaussian/x	weighted average	unweighted average
tert +/+ #1	94:1:296 (3000-10000)	100	0.95	6876.9	6813.7-6940	1752.4	1708.9-1798.2	6396.8	6374.5	6876.9
tert +/+ #2	78:1:296 (3000-11000)	100	0.95	7298.4	7241.4-7355.4	1978.1	1938.7-2019.3	6715.8	6726.9	7298.4
tert +/+ #3	94:1:296 (3000-10000)	100	0.95	6857.4	6790.1-6924.8	1651.5	1605.2-1700.5	6433.5	6417.9	6857.4
tert +/- #1	113:1:255 (3800-8900)	100	0.95	6795.7	6750-6841.4	1216.1	1184.6-12493	6570.6	6554.2	6795.7
tert +/- #2	107:1:228 (4500-9200)	100	95%	7067.2	7023.5-7111.1	1211.3	1181.2-1243.1	6853.1	6849.3	7067.2
tert +/- #3	113:1:296 (3000-9000)	100	95%	6588.6	6542.7-66345	13642	1332.5-1397.5	6292.9	6253.8	6588.6
tert -/- #1	113:1:296 (3000-9000)	100	0.95	6433.5	6389-6477.9	1330.5	1299.8-1362.7	6145.4	6126	6433.5
tert -/- #2	113:1:296 (3000-9000)	100	0.95	6185.7	6141.1-6230.4	1410.7	1379.8-1443	5845.3	5833.6	6185.7
tert -/- #3	113:1:363 (2000-9000)	100	0.95	6025	5976.7-6073.3	1592.1	1558.6-1627.0	5569.9	5520.3	6025

Set 1 - high MW range

name	range	bar range	confidence level	υ	conf interval υ	σ	conf interval σ	x for y max from Gaussian/x	weighted average	unweighted average
tert +/+ #1	15:1:65 (12000-15000)	100	0.95	13726	13682-13769	1030	1000.2-1061.6	13648	13650	13726
tert +/+ #2	15:1:79 (11000-15000)	100	0.95	13165	13121-13209	1224.5	1194.1-1256.6	13050	13053	13165
tert +/+ #3	15:1:65 (12000-15000)	100	0.95	13783	13740-13825	932	902.97-963.18	13719	13721	13783
tert +/- #1	15:1:65 (12000-15000)	100	0.95	13784	13745-13824	1009.1	981.7-1038	13710	13712	13784
tert +/- #2	32:1:64 (12000-14500)	100	0.95	13246	13216-13276	657.06	636.35-679.18	13213	13213	13246
tert +/- #3	32:1:71 (11500-14500)	100	0.95	13035	13001-13068	772.85	749.84-797.30	12989	12988	13035
tert -/- #1	46:1:57 (12500-13300)	100	0.95	12894	12866-12923	234.91	216.27-257.09	12890	12890	12894
tert -/- #2	46:1:57 (12500-13300)	100	0.95	12925	12897-1295.4	240.93	222.23-263.09	12921	12921	12925
tert -/- #3	46:1:64 (12000-13300)	100	0.95	12628	12602-12653	351.55	334.54-370.39	12618	12618	12628

Figure S4: Tables of results and range used after setting the upper and lower background for Set 1 TRF analysis.

Set 2 - low MW range

name	range	bar range	confidence level	υ	conf interval υ	σ	conf interval σ	x for y max from Gaussian/x	weighted average	unweighted average
tert +/+ #1	54:l:280 (3000-11500)	100	0.95	7703	7645.3-7760.8	1964.8	1924.9-2006.5	7164.2	7174.9	7703
tert +/+ #2	61:1:280 (3000-11000)	100	0.95	7620.4	7564.2-7676.6	1753.9	1715.1-1794.6	7192.7	7160.2	7620.4
tert +/+ #3	54:1:280 (3000-11500)	100	0.95	7595.9	7523.1-7668.6	2027.3	1977.1-2080	7009.5	7004.9	7595.9
tert +/- #1	77:1:280 (3000-10000)	100	0.95	728.6	7168.3-7268.8	1499	1464.4-1535.4	6892.6	6859.4	7218.6
tert +/- #2	77:1:280 (3000-10000)	100	0.95	7382	7332.8-7431.2	1530.8	1496.8-1566.4	7049.6	7001.4	7382
tert +/- #3	77:1:280 (3000-10000)	100	0.95	7017.1	6962.2-7072	1683.5	1645.6-1723.3	6586.8	6554.3	7017.1
tert -/- #1	77:1:280 (3000-10000)	100	0.95	6924.3	6875.5-6973.1	1554	1520.3-1589.3	6555.9	6538.1	6924.3
tert -/- #2	94:1:280 (3000-10000)	100	0.95	6399.4	6355.4-6443.4	1391.9	1361.5-1423.8	6080.8	6062.4	6399.4
tert -/- #3	94:1:280 (3000-10000)	100	0.95	6252.2	6207-6297.3	1437	1405.8-1469.6	5902.3	5887.4	6252.2

Set 2 - high MW range

name	range	bar range	confidence level	υ	conf interval υ	σ	conf interval σ	x for y max from Gaussian/x	weighted average	unweighted average
tert +/+ #1	9:1:55 (11500-15000)	100	0.95	13291	13252-13329	901.55	875.44-929.28	13229	13229	13291
tert +/+ #2	9:1:41 (12500-15000)	100	0.95	13745	13714-13777	634.13	612.87-656.94	13716	13716	13745
tert +/+ #3	9:1:41 (12500-15000)	100	0.95	13759	13726-13792	619.61	597.08-643.91	13731	13731	13759
tert +/- #1	9:1:48 (12000-15000)	100	0.95	13449	13415-13483	764.63	741.49-789.27	13405	13405	13449
tert +/- #2	9:1:48 (12000-15000)	100	0.95	13515	13480-13550	799.84	775.71-825.52	13467	13467	13515
tert +/- #3	9:1:48 (12000-15000)	100	0.95	13606	13571-13641	783.52	759.45-809.17	13561	13560	13606
tert -/- #1	27:1:41 (12500-13500)	100	0.95	12993	12957-13029	299.09	275.62-326.96	12986	12986	12993
tert -/- #2	27:1:41 (12500-13500)	100	0.95	13022	12991-13053	291.39	271.03-315.08	13015	13015	13022
tert -/- #3	27:1:48 (12000-13500)	100	0.95	12690	12657-12723	413.99	392.06-438.54	12676	12676	12690

Figure S 5: Tables of results and range used after setting the upper and lower background for Set 2 TRF analysis.